Bioactive potency of extracts from *Stylissa carteri* and *Amphimedon chloros* with silver nanoparticles against cancer cell lines and pathogenic bacteria

MOATH ALQARALEH[1], KHALED M. KHLEIFAT[2], ALI AL-SAMYDAI[3], BELAL O. AL-NAJJAR[3], FADI G. SAQALLAH[4], YASEEN T. AL QAISI[5], AHMAD Z. ALSARAYREH[5], DANA A. ALQUDAH[6] and ABDULFATTAH S. FARARJEH[1]

[1]Department of Medical Laboratory Sciences, Faculty of Allied Medical Sciences, Al-Balqa Applied University, Al-Salt 19117, Jordan; [2]Department of Medical Laboratory Sciences, Faculty of Science, Mutah University, Al-Karak 61710, Jordan; [3]Department of Pharmaceutical and Pharmaceutical Technology, Faculty of Pharmacy, Pharmacological and Diagnostic Research Center, Al-Ahliyya Amman University, Amman 11814, Jordan; [4]Department of Pharmacy, Faculty of Pharmacy, Al-Zaytoonah University of Jordan, Amman 11733, Jordan; [5]Department of Biological Sciences, Faculty of Science, Mutah University, Al-Karak 61710, Jordan; [6]Department of Pharmaceutics and Technology, Cell Therapy Center, The University of Jordan, Amman 11942, Jordan

Received May 17, 2024; Accepted October 15, 2024

DOI: 10.3892/br.2024.1912

Abstract. Silver nanoparticles (AgNPs) are spherical particles with a number of specific and unique physical (such as surface plasmon resonance, high electrical conductivity and thermal stability) as well as chemical (including antimicrobial activity, catalytic efficiency and the ability to form conjugates with biomolecules) properties. These properties allow AgNPs to exhibit desired interactions with the biological system and make them prospective candidates for use in antibacterial and anticancer activities. AgNPs have a quenching capacity, which produces reactive oxygen species and disrupts cellular processes (such as reducing the function of the mitochondria, damaging the cell membrane, inhibiting DNA replication and altering protein synthesis). In addition, sponge extracts contain biologically active substances with therapeutic effects. Therefore, the concurrent use of these agents may present a potential for the development of novel antitumor and antimicrobial drugs. The present study investigated the cytotoxic effects of AgNPs combined with the extracts from sponge species, *Stylissa carteri* or *Amphimedon chloros*, against various cancer cell lines and pathogenic bacterial strains. The present study was novel as it provided a further understanding of the cytotoxicity and underlying mechanisms of AgNPs. Alterations in the properties, such as size, charge and polydispersity index, of the AgNPs were demonstrated after lyophilization. Scanning electron microscopy revealed submicron-sized particles. The cytotoxic potential of AgNPs across various cancer cell lines such as lung, colorectal, breast and pancreatic cancer cell lines, was demonstrated, especially when the AgNPs were combined with sponge extracts, which suggested a synergistic effect. Analysis using liquid chromatography-mass spectrometry revealed key chemical components in the extracts, and molecular docking simulations indicated potential inhibition interactions between a number of the extract components and the epidermal growth factor receptor and tyrosine kinase receptor A. Synergistic antibacterial effects against several bacterial species such as *Staphylococcus xylosus*, *Klebsiella oxytoca*, *Enterobacter aerogenes*, *Micrococcus* spp. and *Escherichia coli*, were observed when AgNPs were combined with sponge ethyl acetate extracts. The results of the present study suggested a potential therapeutic application of marine-derived compounds and nanotechnology in combating cancer and bacterial infections. Future research should further elucidate the mechanistic pathways and investigate the *in vivo* therapeutic efficacy.

Correspondence to: Dr Moath Alqaraleh, Department of Medical Laboratory Sciences, Faculty of Allied Medical Sciences, Al-Balqa Applied University, 443 60th Street, Al-Salt 19117, Jordan
E-mail: muath.garalleh@bau.edu.jo

Abbreviations: AgNPs, silver nanoparticles; DMEM, Dulbecco's Modified Eagle Medium; DMSO, dimethyl sulfoxide; EGFR, epidermal growth factor receptor; FBS, fetal bovine serum; LC-MS, liquid chromatography-mass spectrometry; PDI, polydispersity index; TrkA, tyrosine kinase receptor A

Key words: Stylissa carteri, *Amphimedon chloros*, AgNPs, EGFR inhibition, TrkA inhibition, antibacterial activity

Introduction

Cancer encompasses a range of conditions marked by an unregulated cell proliferation that infiltrates into nearby tissues, and potentially metastasizes to distant areas of the body (1). Despite progress in cancer treatment, it remains a worldwide major health issue. In 2023, the United States reported 1,958,310 new cases of cancer and 609,820 mortalities (2).

Jordan also faces a similar challenge, and reported 11,559 new cases and 6,190 mortalities in 2023. Furthermore, patients are mainly diagnosed with breast (20%), colorectal (11.6%) and lung cancer (7.4%) (2).

Cancer treatment predominantly relies on conventional chemotherapy, which uses a combination of drugs (such as 5-fluorouracil, leucovorin, oxaliplatin and irinotecan) alongside surgical procedures and radiation therapy (3). The development of resistance towards these conventional chemotherapy agents reduces their effectiveness, resulting in only minimal and temporary advantages (4). However, the process of developing novel drugs has considerable challenges, including high financial burdens, extensive clinical trials and rigorous regulatory demands (5).

Nanomedicine is an emerging discipline and focuses on using nano-sized materials as biomedical tools for both diagnosis and treatment purposes, especially within oncology (6). This approach is gaining interest as a preferred method over chemotherapy drugs due to its enhanced safety and efficacy (7). It facilitates the amalgamation of drugs with synergistic effects, potentially enhancing treatment efficacy, reducing adverse effects and mitigating the emergence of drug resistance (8,9). These multifaceted benefits render the use of nano-scaled carriers and drugs a progressively favored option over conventional therapies, particularly in addressing diseases such as cancer (10-17).

Silver nanoparticles (AgNPs) have gained attention within pharmaceutical and medical settings due to having antimicrobial properties and inducing cytotoxicity in diverse cancer cell lines such as colorectal and breast cancer cell lines (18,19). AgNPs exhibit multifaceted applications in the research and therapy of cancer. They are utilized primarily as effective drug delivery systems, encapsulating anticancer agents (such as methotrexate, imatinib, doxorubicin and gemcitabine) to enhance their targeting and efficacy against tumors while minimizing systematic side effects (20). AgNPs themselves possess intrinsic anticancer properties through mechanisms such as the induction of apoptosis and disruption of cellular signaling pathways in cancer cells (21). Furthermore, AgNPs are used in diagnostics by functionalizing their surfaces with specific biomolecules (such as aptamer or specific antibodies) that bind to cancer biomarkers [such as platelet-derived growth factors, human epidermal growth factor receptor (EGFR) 2 and prostate-specific antigen], resulting in sensitive detection methods (22). Additionally, AgNPs are radiosensitizers and increase the effectiveness of radiotherapy by enhancing the DNA damage in cancer cells (23). These diverse applications highlight the potential for AgNPs to advance cancer treatment modalities through targeted drug delivery, diagnostic and therapeutic interventions.

Bioactive components sourced from a variety of organisms, including plants and animals, offer anticancer and various other biological effects, presenting opportunities for the development of pharmaceutical products (24-27). Phytoestrogens and Rhizoma polygonati exhibit anticancer and antiaging properties (28,29). *Tribulus terrestris* indicates a potential for neuroprotection, and may be a treatment option for cognitive disorders such as Parkinson's and Alzheimer's disease (30), while camel milk whey protein hydrolysates provide anti-inflammatory and anticancer benefits (31). Furthermore, actinobacterial agents (such as indole-3-acetic acid, polyamines and 1-aminocyclopropane-1-carboxylic acid deaminase) from *Salicornia bigelovii* indicate a potential for enhancing agricultural productivity, such as enhancing the root biomass, increasing the yield of the seeds and increasing the tolerance of plants to saline soil (32). Additionally, sea sponges in particular have shown antioxidant and anti-inflammatory properties, which reduce the risk of cancer (33).

Stylissa carteri and *Amphimedon chloros*, marine sponges that inhabit the exclusive economic zone of Indonesia, have gained attention for their therapeutic properties, particularly their potential in the treatment of cancer (34,35). The present study aimed to investigate the cytotoxic effects of AgNPs with extracts of *Stylissa carteri* or *Amphimedon chloros*, collected from the Red Sea coastline, against various types of cancer and bacterial strains. To the best of our knowledge, the present study was the first to conduct an evaluation of the cytotoxicity of *Stylissa carteri* and *Amphimedon chloros*.

Materials and methods

Materials. L-glutamine-containing Dulbecco's Modified Eagle Medium (DMEM), penicillin/streptomycin and fetal bovine serum (FBS) were purchased from EuroClone SpA. Both phosphate buffer saline and trypsin were purchased from Thermo Fisher Scientific, Inc. Ethyl acetate was purchased from Sigma-Aldrich; Merck KGaA. The MTT reagent the stop solution [dimethyl sulfoxide (DMSO)] and trypan blue dye were provided by Promega Corporation. Flow tubes (BD Biosciences) were used for centrifugation. BD FACSDiva™ software (version 8.0; BD Biosciences) and StemPro™ Accutase™ Cell Dissociation Reagent (Gibco; Thermo Fisher Scientific, Inc.) were used in the present study.

Biosynthesis of AgNPs using Aspergillus flavus. In the present study, AgNPs were synthesized using *Aspergillus flavus* strain MG973280, which was obtain from American Type Culture Collection (ATCC). The fungal culture was prepared as previously described (36). Briefly, *Aspergillus flavus* spores were adjusted to a concentration of $2.0x10^6$ and cultivated in a complex broth medium that included 10 g/l glucose, 10 g/l yeast extract and 5 g/l NaCl (pH 7). Subsequently, the culture was incubated for 72 h at 33˚C and cells were agitated using an orbital shaker at 0.10 x g. Whatman® grade 1 filter paper was used to filter the culture at the end of the incubation period. The resultant mycelia, or biomass, were then collected and washed with deionized distilled water.

To produce AgNPs using the fungal biomass, the method reported in the study by Jadidev and Narasimha (37) was followed with minor adjustments. Briefly, 10 g of the first crude biomass were agitated using an orbital shaker at 0.10 x g for 72 h while submerged in 100 ml of sterile deionized water at 33˚C and pH 7.0. After the crude biomass was filtered using Whatman® grade 1 filter paper, the resulting suspension containing the fungal filtrate without biomass was collected. Subsequently, 100 ml of this biomass-free fungal filtrate was combined with 1 mM of silver nitrate to produce AgNPs. The mixtures were then continuously stirred in the dark at 27˚C for 72 h using a magnetic stirrer.

Morphology and particle size analysis. NPs were lyophilized at -54˚C and 0.2 mbar for 24 h using a Lyovapor L-200 freeze dryer (BUCHI UK Ltd.). Scanning electron microscope (SEM) images were obtained at 200 kV using a JEM-2010 microscope (JEOL, Ltd.) in order to analyze the surface morphology of the AgNPs. The powdered samples were coated with gold using sputter coater and a carbon thread coater (Leica Biosystems). The resulting particle size was measured using the Zetasizer Nano ZSP (Malvern Panalytical, Ltd.).

Sponge collection and identification. Sponge samples were gathered from several locations in the Gulf of Aqaba (29˚27' N, 34˚58' E) by specialists from the Marine Science Station at the University of Jordan (Aqaba, Jordan). The sponges were found by divers between the depths of 1-18 meters. After being cleared of debris, the samples were frozen at -80˚C, and then sent in sealed sterile polyethylene containers (which were submerged in seawater in order to maintain a moist environment during transport) to Aqaba International Laboratories-BEN HAYYAN for freeze-drying and extraction. Using specified morphological traits listed in the Systema Porifera and World Porifera Database (35,38-42), the sponges, *Stylissa carteri* and *Amphimedon chloros*, were identified.

Extraction of sponge extracts. Sponge fragments were weighed, freeze-dried for 48 h at -40˚C and then ground into a powder. The powder (weighing 45.0-350.0 g) was soaked at room temperature for 48 h in a 1:1 mixture of methanol and dichloromethane. Subsequently, a lyophilizer was used to filter and dehydrate the solution. The final pure extract was divided into non-polar, semi-polar and polar components by dispersing it in distilled water and using n-hexane and ethyl acetate as partitioning agents. The pure extract from each solvent was labeled and kept frozen at -20˚C (43,44).

Cancer cell lines culture. In the present study, to investigate the anticancer activity of the candidate mixtures, four cancer cell lines were used: i) A human lung cancer cell line (A549; cat. no. CCL-185; ATCC); ii) a human colorectal cancer cell line (HT-29; cat. no. HTB-38; ATCC); iii) a human breast cancer cell line (MCF7; cat. no. HTB-22; ATCC); and iv) a pancreatic cancer cell line (PANC-1; cat. no. CRL-1469; ATCC). For selective purposes, a normal human umbilical vein endothelial cell line (HUVEC; cat. no. CRL-1730; ATCC) was used. All of the cell lines, were cultured in DMEM containing 10% FBS, 10 mM HEPES buffer, 100 μg/ml L-glutamine, 50 μg/ml gentamicin, 100 μg/ml penicillin and 100 mg/ml streptomycin. ATCC provided authenticated cell lines, which ensured that the cell lines were correctly identified and contamination-free. Additionally, mycoplasma testing was performed on all of the cell lines used in the present study, which confirmed the absence of mycoplasma contamination.

Colorimetric MTT assay. A colorimetric MTT assay was used to evaluate the viability of the cells. Each type of cell line was seeded in 96-well plates at a density of $1x10^4$ cells per well and cultured for 24 h at 37˚C (45). Subsequently, the cells were treated with: i) The extracts of each of the sponge species, *Stylissa carteri* and *Amphimedon chloros,* separately at concentrations ranging from 6-200 μg/ml; ii) AgNPs at concentrations ranging from 0.75-200 μg/ml; or iii) mixtures of 0.75 μg/ml AgNPs with extracts of *Stylissa carteri* or *Amphimedon chloros* at concentrations ranging from 6-200 μg/ml. Following a 72-h incubation period at 37˚C (46), 15 μl of MTT solution was added to each well, and then the plates were incubated at 37˚C for 4 h. Subsequently, 100 μl of DMSO was added to each well to dissolve the formed formazan crystal. The BioTek ELx800™ microplate reader was then used to measure the optical density at 590/630 nm to assess cell growth.

Screening and identifying compounds from the sponge extracts using liquid chromatography-mass spectrometry (LC-MS). LC-MS is an analytical method that combines MS and LC. LC separates components of a mixture by passing them through a chromatographic column. Even when LC is unable to positively identify these separated components, MS can be used to identify both known and unknown chemicals and provide information on their structures (47).

A mobile phase comprising solvents A and B in a gradient was used in the LC-MS analysis. Solvent A consisted of formic acid dissolved in water at a concentration of 0.1% (v/v), and solvent B consisted of formic acid dissolved in acetonitrile at the same concentration. The experimental parameters used included an Agilent Zorbax Eclipse XDB-C18 column (Agilent Technologies, Inc.) measuring 2.1x150 mm x3.5 μm, a temperature maintained at 25˚C, the sponge extract dissolved in methanol at a concentration of 18 mg/ml and an injection volume of 1 μl. The sample was injectedinto the LC-MS system, which included the following components: A mass detector using a SIL-30AC autosampler with a cooler, a Shimadzu CBM-20A system controller, an LC-30AD pump, a CTO-30 column oven and an electrospray ion-mass spectrometer with a skimmer voltage of 65 V and a fragmentor voltage of 125 V, all components were of the Shimadzu LC-MS 8030 (Shimadzu Corporation). Nitrogen gas with 99.99% purity and a flow rate of 10 l/min served as the drying gas during operation in positive ion mode. Additionally, a nebulizer operating at a pressure of 45 psi and a capillary temperature of 350˚C were used. Subsequently, the mass/number of ions of the eluent was scanned from positions 100-1,000. Authentic standard substances were used for result validation.

Molecular docking. Molecular docking simulations were performed using tyrosine kinase receptor A [TrkA; Protein Data Bank (PDB) ID, 7VKO; https://www.rcsb.org/structure/7VKO] (48) and an EGFR kinase domain (PDB ID, 4I23; https://www.rcsb.org/structure/4i23) (49) in order to investigate the binding affinities of the major components in *Stylissa carteri* or *Amphimedon chloros*. AutoDock (version 4.2.6) (50,51) was used according the methods described in the studies by Saqallah *et al* (52) and Shtaiwi *et al* (53) with slight modifications. Briefly, all protein structures were prepared using BIOVIA® Discovery Studio® (version 16.1) (54) by removing water molecules (if applicable) and complexed co-structures. Complexed inhibitors (dacomitinib and repotrectinib in the EGFR kinase domain and TrkA structures, respectively) were separated from the crystal structures to be used as control ligands. Using AutoDockTools

(version 1.5.6) (50), Kollman charges and polar hydrogen atoms were assigned to the proteins. Additionally, the 3D conformers of the compounds identified in the sponge extracts were downloaded from the NCBI PubChem database (pubchem.ncbi.nlm.nih.gov) and Gasteiger charges were assigned accordingly. A grid box with the size of 153 Å was set with the coordinates of -0.697, -52.750, -23.233 as x, y, z, respectively, for the EGFR kinase domain protein, and with the same size at -18.081, -43.125, -13.177 as x, y, z, respectively, for the TrkA protein. Simulations were carried out using 100 Lamarckian Genetic Algorithm runs with default parameters. Conformations with the lowest free energy of binding and the most populated cluster were selected for further analysis. Analyses of the interactions were carried out using BIOVIA® Discovery Studio® (version 16.1).

Isolation of the bacterial strains utilized in antibacterial studies. To study the antibacterial activity of the sponge-AgNPs mixtures, bacterial cells were obtained from hydatid cyst fluid sourced from various affected anatomical sites, such as the liver and lung, and five different isolated bacterial species were obtained in a previous study by Al Qaisi *et al* (55). The bacterial species used in the present study were *Staphylococcus xylosus*, *Klebsiella oxytoca*, *Enterobacter aerogenes*, *Micrococcus* spp. and *Escherichia coli*. *Pseudomonas aeruginosa* (cat. no. 27853; ATCC) was used as a control. The isolates were preserved on nutrient agar slants at 4˚C for up to 1 month.

Antibacterial agar disc diffusion assay. Isolated bacteria were first cultured in Muller Hinton Broth at 37˚C for 24 h for activation before carrying out the antibacterial tests. The antibacterial activity of the sponge extracts and AgNPs were measured using Muller Hinton agar and the disc diffusion method. Inhibitory zone diameters were calculated in mm (56). Briefly, 20 μg of sponge extract (either from *Stylissa carteri* or *Amphimedon chloros*) or AgNPs were used to impregnate sterile filter paper discs, which were then put on inoculated Petri dishes containing 0.1 ml of a bacterial solution containing $1.5x10^8$ colony forming units/ml. Discs pre-dosed with 50 g/ml chloramphenicol and 50 g/ml ampicillin were used as positive controls, while discs containing 5% DMSO served as negative controls. After 24 h of incubation at 37˚C, the diameters of the inhibition zones around the extract-impregnated discs were measured and compared with those of the controls. To identify active and inactive sponge preparations, the inhibition zone diameter was used as a metric. Each sample was tested three times. To test for sponge extract-AgNP synergy, two different concentrations were used, which were 10 μg sponge extract and 10 μg AgNPs/disc, and 10 μg sponge extract and 5 μg AgNPs/disc (57).

Statistical analysis. Results from three or four independent experiments are presented as the means ± standard deviation. Statistical variances between the control group and various treatment groups were evaluated using GraphPad Prism version 10 (Dotmatics). Results were analyzed using one-way ANOVA followed by the Dunnett's test, or using an unpaired t-test. $P<0.05$ was considered to indicate a statistically significant difference.

Results

Lyophilization alters the size, charge and stability of AgNPs. A significant difference in charge, but not in size and polydispersity index (PDI) between the pre-and post-lyophilization states are presented in Fig. 1. Before lyophilization, the mean charge was-25.30±0.28 mV, the mean size was 108.65±3.45 nm and the PDI was 0.27±0.07. After the process of lyophilization, the mean size increased to 171.60±13.01 nm, the mean charge increased to -15.05±0.01 mV and the PDI increased to 0.34±0.01. Although all measurements for nanoparticle size (ideal range, 50-200 nm), charge (ideal range, -10 to -30 mV) and PDI (ideal range, ≤0.5) remained within the ideal ranges, these differences indicated that the lyophilization process did not significantly affect the properties of the AgNPs.

SEM analysis reveals uniform distribution and nanoscale size of the AgNPs with minimal aggregation. To investigate the produced AgNPs, SEM was used (Fig. 2). The AgNPs had a uniform distribution and an approximately spherical shape, with negligible aggregation, which indicated a stable production process. Based on the 200 nm scale bar, the majority of the particles had a diameter of <100 nm, which indicated that the size distribution was in the nanoscale zone. Particle aggregation occurs frequently in nanoparticle samples (58); however, in the present study, only minimal aggregation was observed, which indicated high dispersion stability. The AgNPs appeared to have a smooth surface, which is consistent with the nature of nanoparticles made using chemical reduction techniques (59,60). These features implied that these AgNPs were suitable for various applications including anticancer and antimicrobial activity.

AgNPs with sponge extracts reveal selective cytotoxicity when using the HUVEC normal cell line. To investigate the selective cytotoxicity of AgNPs on the HUVEC normal cell line, an MTT assay was carried out. Cytotoxicity was observed across concentrations ranging from 0.75-200 μg/ml of AgNPs (Fig. 3A). There was a significant difference in the cell cytotoxicity between the 0.75 and 3 μg/ml AgNPs (Fig. 3A), which indicated that 3 μg/ml AgNPs had a lower cytotoxicity compared with 0.75 μg/ml AgNPs in the HUVEC normal cell line. However, 0.75 μg/ml AgNPs were used in the subsequent experiments based on several factors, such as to prevent drug resistance. An advantage of combination therapy is the prevention of drug resistance, which often occurs when high doses of a single agent are used repeatedly (61); therefore, using a lower concentration (0.75 μg/ml) of AgNPs avoided a high-dose exposure, which could otherwise lead to resistance. Additionally, lower doses of nanoparticles may be preferable for long-term use in order to minimize potential side effects while still retaining efficacy (62). Therefore, the subsequent combination experiments used *Stylissa carteri* or *Amphimedon chloros* extracts with 0.75 μg/ml AgNPs to minimize the cytotoxic effect of the AgNPs on the HUVEC normal cell line while maximizing the cytotoxic potential against various cancer cell lines. Fig. 3B presents the cytotoxic effects of *Stylissa carteri* extract alone and in combination with 0.75 μg/ml AgNPs. Fig. 3C presents the cytotoxicity of *Amphimedon chloros* extract alone and in combination with 0.75 μg/ml AgNPs. The results indicated a significant reduction in HUVEC cytotoxicity

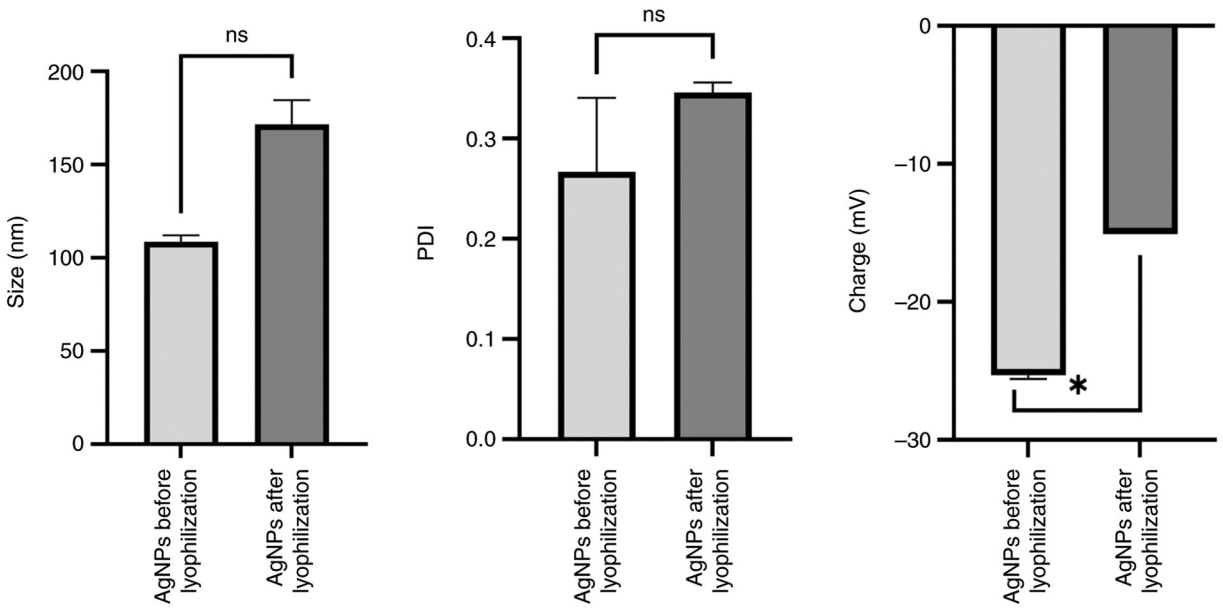

Figure 1. Size, PDI and surface charge of AgNPs before and after lyophilization. While there was not a significant difference in the size and PDI of the AgNPs before and after lypophilization, a significant difference in the surface charge was revealed after lyophilization. The results are presented as means ± SD (n=3). *P<0.05. AgNPs, silver nanoparticles; PDI, polydispersity index; ns, not significant.

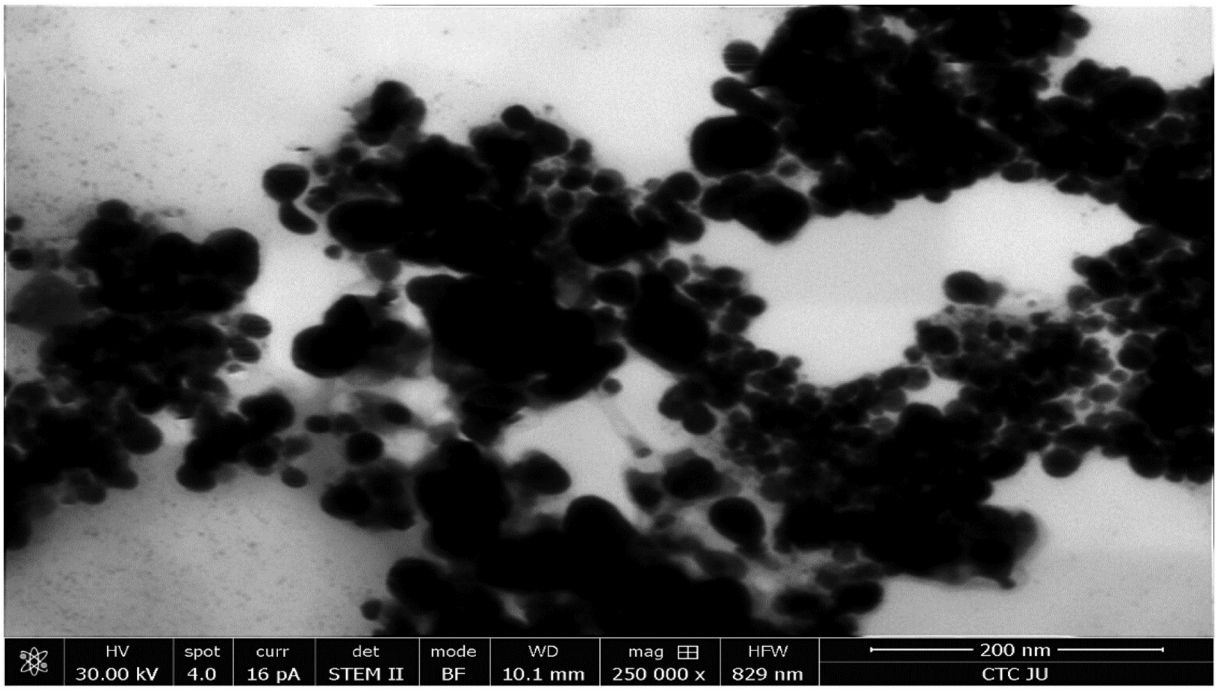

Figure 2. SEM micrograph of AgNPs. A high-resolution SEM image of the morphology and distribution of AgNPs, which were synthesized using 1.0 mM silver nitrate and the fungus *Aspergillus flavus*. SEM, scanning electron microscopy; AgNPs, silver nanoparticles; HV, high voltage (accelerating voltage in kV applied to the microscope); spot, spot size (beam diameter for optimal resolution); pA, picoamperes; curr, current (electron beam current in pA); det, detector (type of detector used to capture the image); STEM II, scanning transmission electron microscopy secondary image; BF, bright field (imaging mode providing high-contrast details in transmission images); WD, working distance (distance between sample surface and objective lens); mag, magnification; HFW, horizontal field width; CTC JU, Cells Therapy Center, Jordan University.

when the *Amphimedon chloros* extract was combined with AgNPs compared with the *Amphimedon chloros* extract alone.

Enhancement of the cytotoxicity of AgNPs with sponge extracts when using the A549 cell line. Fig. 4A demonstrates the cytotoxic impact of the AgNPs on the A549 cell line. The results revealed a significant increase in the cytotoxicity within the concentration range of 1.5-200 μg/ml AgNPs compared with the concentration of 0.75 μg/ml AgNPs. Fig. 4B presents the cytotoxicity of the *Stylissa carteri* extract alone and in combination with 0.75 μg/ml AgNPs. Fig. 4C presents the cytotoxic effects of the *Amphimedon chloros* extract alone and

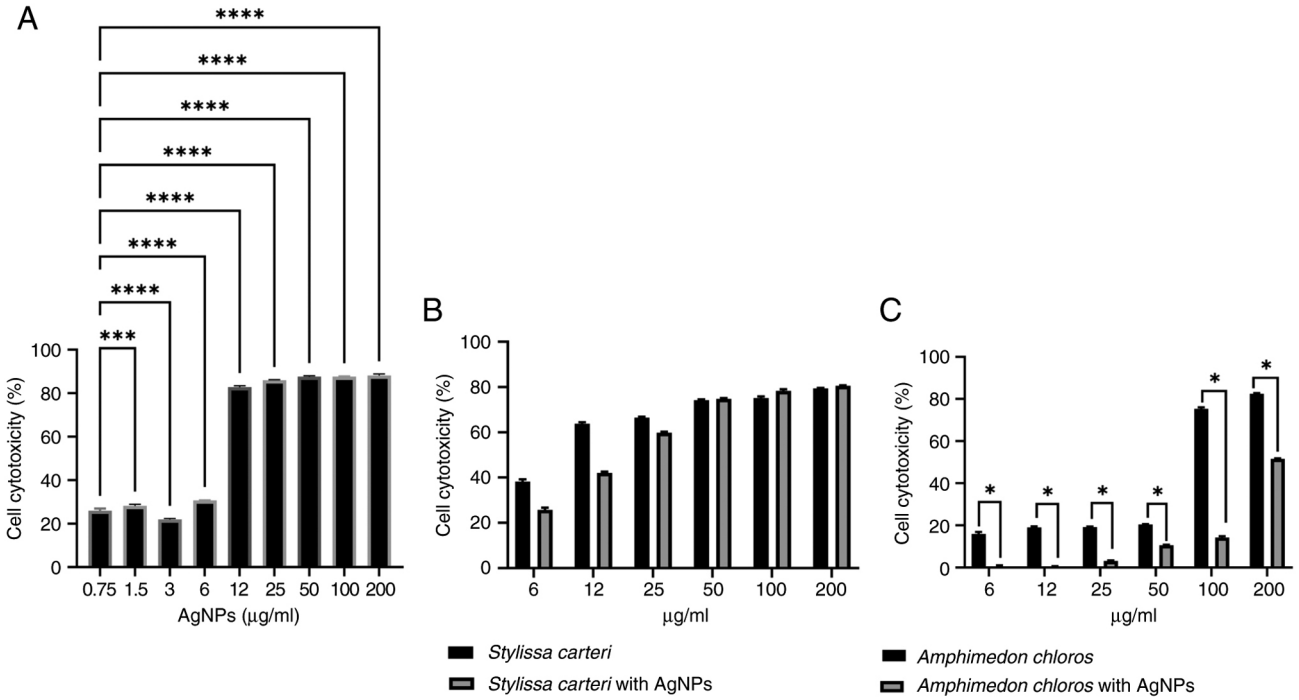

Figure 3. Cytotoxicity of HUVEC cells to AgNPs, *Stylissa carteri* and *Amphimedon chloros*. (A) Cytotoxicity of different concentrations of AgNPs on the HUVEC cell line (analyzed using one-way ANOVA followed by the Dunnett's test). Cytotoxicity of (B) the *Stylissa carteri* extract alone and in combination with 0.75 µg/ml AgNPs and (C) the *Amphimedon chloros* extract alone and in combination with 0.75 µg/ml AgNPs on the endothelial HUVEC cell line (analyzed using unpaired t-tests). The results are presented as means ± SD (n=3). *P<0.05, ***P<0.001 and ****P<0.0001. AgNPs, silver nanoparticles; HUVEC, human umbilical vein endothelial cell line.

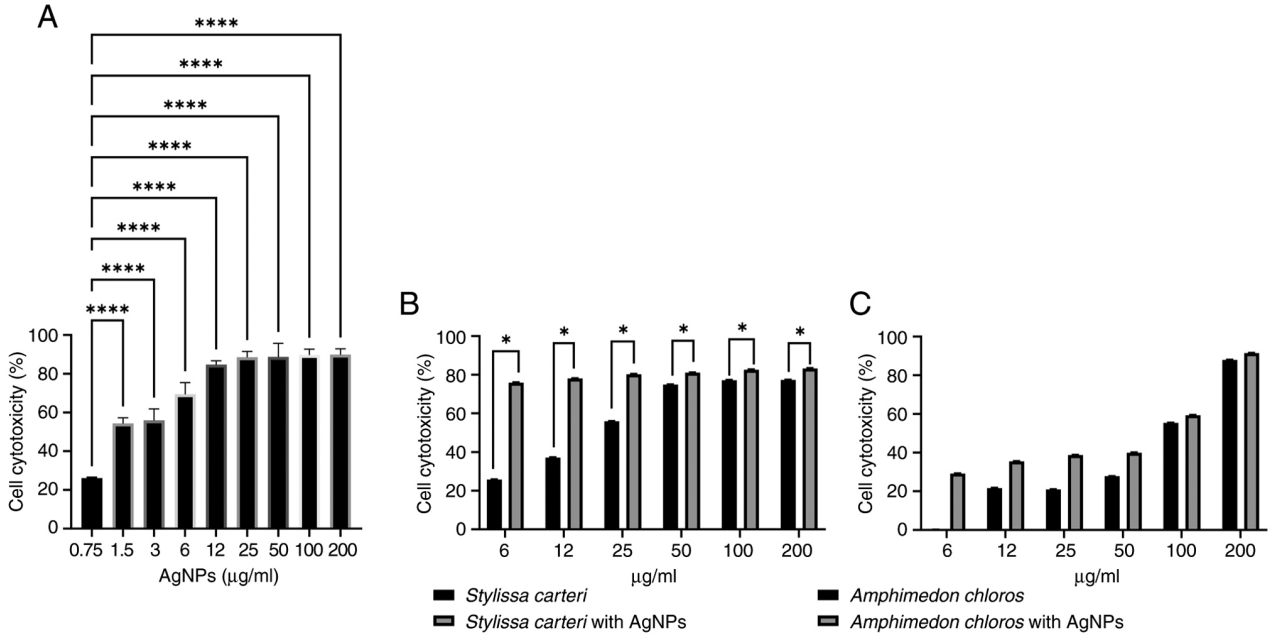

Figure 4. Cytotoxicity of A549 cells to AgNPs, *Stylissa carteri* and *Amphimedon chloros*. (A) Cytotoxicity of different concentrations of AgNPs on the lung cancer A549 cell line (analyzed using one-way ANOVA followed by the Dunnett's test). Cytotoxicity of (B) the *Stylissa carteri* extract alone and in combination with 0.75 µg/ml AgNPs and (C) the *Amphimedon chloros* extract alone and in combination with 0.75 µg/ml AgNPs on the lung cancer A549 cell line (analyzed using unpaired t-tests). The results are presented as means ± SD (n=3). *P<0.05 and ****P<0.0001. AgNPs, silver nanoparticles.

in combination with 0.75 µg/ml AgNPs. The results revealed a significant augmentation in the A549 cell cytotoxicity when the *Stylissa carteri* extract was co-administered with 0.75 µg/ml AgNPs compared with the cytotoxic effects of the *Stylissa carteri* extract alone.

Neither of the sponge extracts significantly increase the cytotoxicity of the AgNPs when using the MCF7 cell line. Fig. 5A demonstrates the cytotoxic effects of the AgNPs on the MCF7 cell line. The results revealed a significant increase in the cytotoxicity within the concentration range of 1.5-200 µg/ml

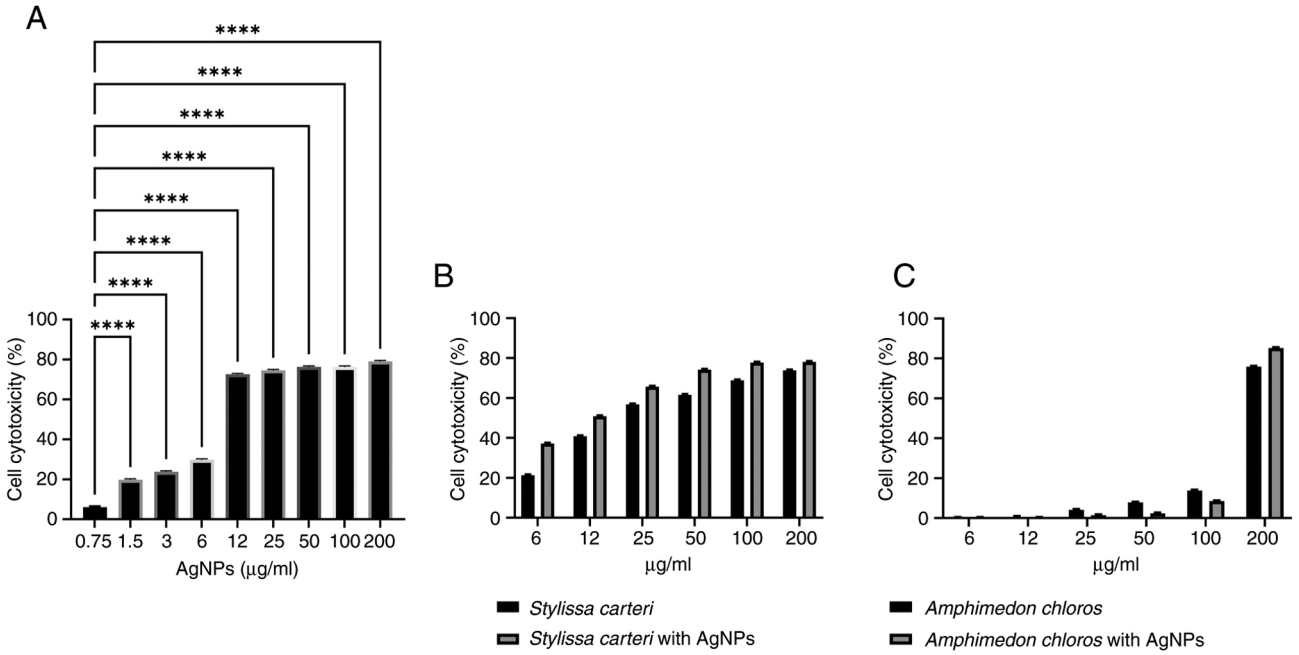

Figure 5. Cytotoxicity of MCF7 cells to AgNPs, *Stylissa carteri* and *Amphimedon chloros*. (A) Cytotoxicity of different concentrations of AgNPs on the breast cancer MCF7 cell line (analyzed using one-way ANOVA followed by the Dunnett's test). Cytotoxicity of (B) the *Stylissa carteri* extract alone and in combination with 0.75 µg/ml AgNPs and (C) the *Amphimedon chloros* extract alone and in combination with 0.75 µg/ml AgNPs on the breast cancer MCF7 cell line (analyzed using unpaired t-tests). The results are presented as means ± SD (n=3). ****P<0.0001. AgNPs, silver nanoparticles.

AgNPs compared with the concentration of 0.75 µg/ml AgNPs. Fig. 5B presents the cytotoxicity of the *Stylissa carteri* extract alone and in combination with 0.75 µg/ml AgNPs, and Fig. 5C presents the cytotoxicity of the *Amphimedon chloros* extract alone and in combination with 0.75 µg/ml AgNPs, when using the MCF7 cell line. However, the cytotoxic effects of the *Stylissa carteri* or the *Amphimedon chloros* extract with 0.75 µg/ml AgNPs were not significantly different using the MCF7 cell line compared with the cytotoxic effects of the *Stylissa carteri* or the *Amphimedon chloros* extracts alone, respectively.

Neither of the sponge extracts significantly increase the cytotoxicity of the AgNPs when using the PANC-1 cell line. Using the PANC-1 cell line, there was a significant increase in the cytotoxicity within the concentration range of 1.5-200 µg/ml AgNPs compared with the concentration of 0.75 µg/ml AgNPs (Fig. 6A). Fig. 6B and C presents the cytotoxic effects of the *Stylissa carteri* extract alone and in combination with 0.75 µg/ml AgNPs, along with the cytotoxicity of the *Amphimedon chloros* extract alone and with 0.75 µg/ml AgNPs, when using the PANC-1 cell line. However, the cytotoxic effects of the *Stylissa carteri* or the *Amphimedon chloros* extract with 0.75 µg/ml AgNPs were not significantly different using the PANC-1 cell line compared with the cytotoxic effects of the *Stylissa carteri* or the *Amphimedon chloros* extracts alone, respectively.

Neither of the sponge extracts significantly increase the cytotoxicity of the AgNPs when using the HT-29 cell line. Fig. 7A presents the cytotoxic effects of the AgNPs on the HT-29 cell line across a concentration range of 0.75-200 µg/ml. The results revealed a significant increase in the cytotoxicity within the concentration range of 1.5-200 µg/ml AgNPs compared with the concentration of 0.75 µg/ml AgNPs. Furthermore, a notable increase in the cell cytotoxicity was observed at AgNP concentrations of 12-200 µg/ml. Additionally, Fig. 7B presents the cytotoxicity of the *Stylissa carteri* extract alone and in combination with 0.75 µg/ml AgNPs, and Fig. 7C presents the cytotoxicity of the *Amphimedon chloros* extract alone and in combination with 0.75 µg/ml AgNPs, when using the HT-29 cell line. However, the cytotoxic effects of the *Stylissa carteri* or the *Amphimedon chloros* extract with 0.75 µg/ml AgNPs were not significantly different using the HT-29 cell line compared with the cytotoxic effects of the *Stylissa carteri* or the *Amphimedon chloros* extracts alone, respectively.

LC-MS reveals key bioactive compounds in the sponge extracts, indicating their potential mechanisms of action. LC-MS analysis revealed that there were different chemical components contained in the *Stylissa carteri* and *Amphimedon chloros* extracts (Tables I and II, respectively). Based on the LC-MS analysis, manzacidine A, debromohymenialdisine and hymenialdisine were identified as the major components in the *Stylissa carteri* extract (Fig. 8). Whereas in the *Amphimedon chloros* extract, methoxyhexadecanoic acid, keramaphidin B and hydroxytricosanoic acid were identified as the major components (Fig. 9). The chemical structures of the predicated components contained in the *Stylissa carteri* and the *Amphimedon chloros* extracts are presented in Fig. 10.

Molecular docking reveals strong binding affinities of marine compounds with EGFR and TrkA kinases, highlighting the inhibitory potential of keramaphidin B. The present study investigated the docking interactions of six marine compounds (debromohymenialdisine, hydroxytricosanoic

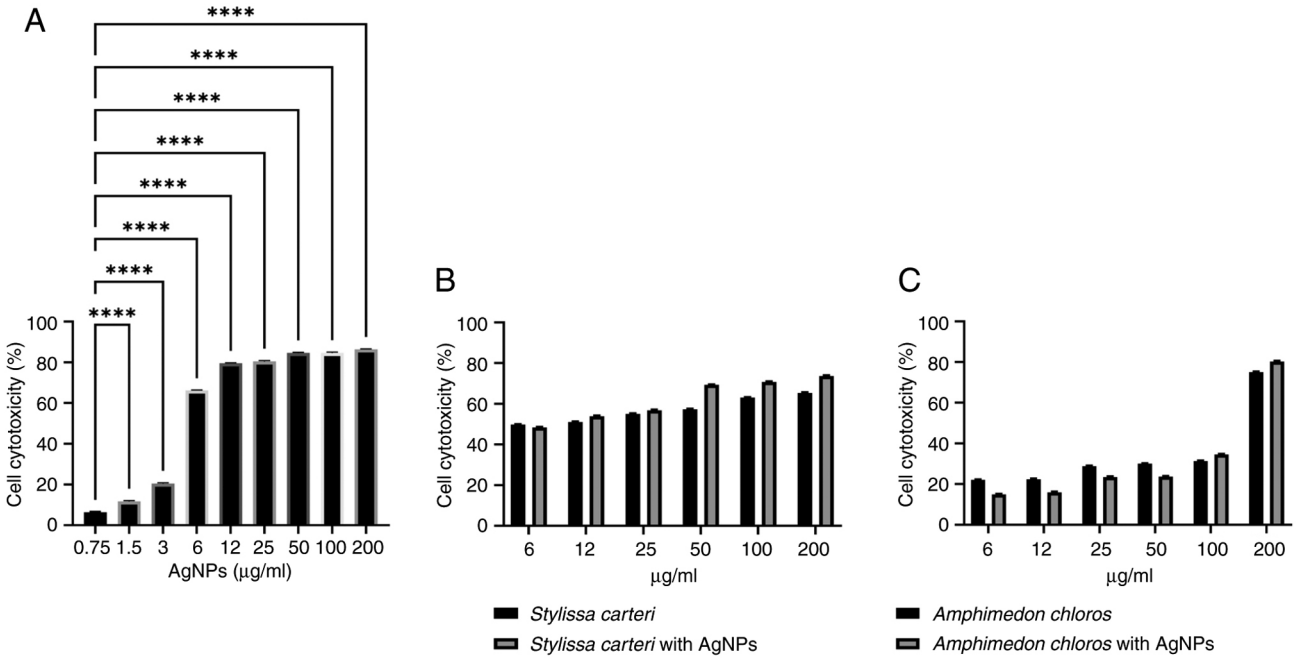

Figure 6. Cytotoxicity of PANC-1 cells to AgNPs, *Stylissa carteri* and *Amphimedon chloros*. (A) Cytotoxicity of different concentrations of AgNPs on the pancreatic cancer PANC-1 cell line (analyzed using one-way ANOVA followed by the Dunnett's test). Cytotoxicity of (B) the *Stylissa carteri* extract alone and in combination with 0.75 µg/ml AgNPs and (C) the *Amphimedon chloros* extract alone and in combination with 0.75 µg/ml AgNPs on the pancreatic cancer PANC-1 cell line (analyzed using unpaired t-tests). The results are presented as means ± SD (n=3). ****P<0.0001. AgNPs, silver nanoparticles.

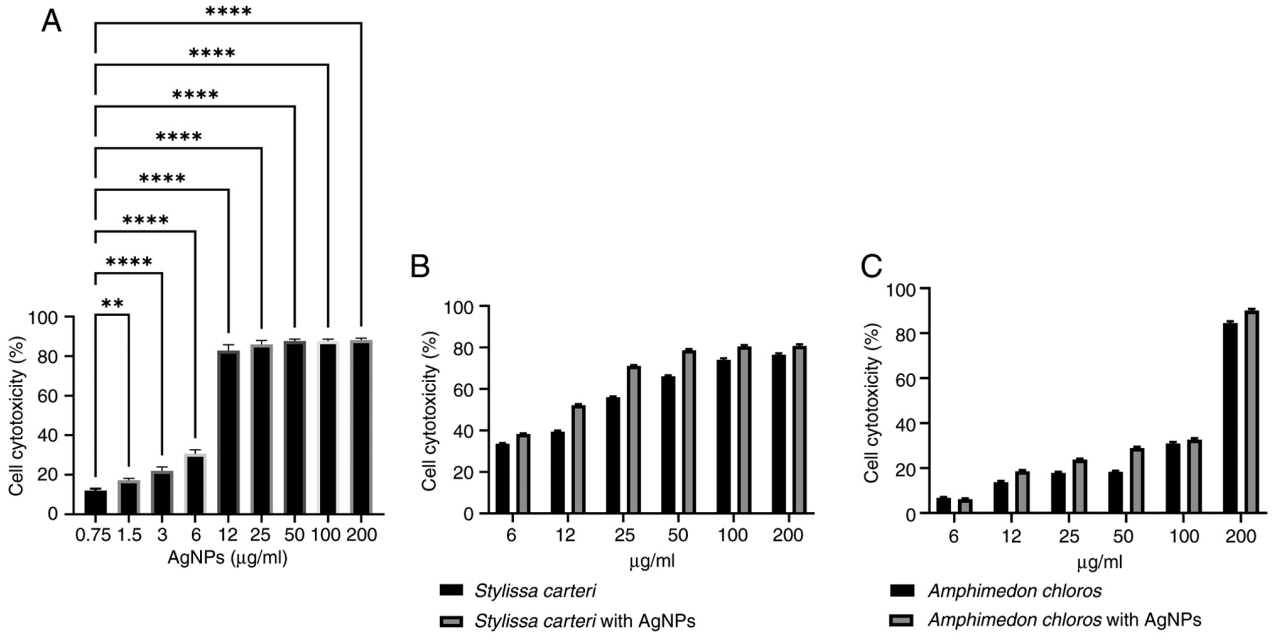

Figure 7. Cytooxicity of HT-29 cells to AgNPs, *Stylissa carteri* and *Amphimedon chloros*. (A) Cytotoxicity of different concentrations of AgNPs on the colorectal cancer HT-29 cell line (analyzed using one-way ANOVA followed by the Dunnett's test). Cytotoxicity of (B) the *Stylissa carteri* extract alone and in combination with 0.75 µg/ml AgNPs and (C) the *Amphimedon chloros* extract alone and in combination with 0.75 µg/ml AgNPs on the colorectal cancer HT-29 cell line (analyzed using unpaired t-tests). The results are presented as means ± SD (n=3). **P<0.01 and ****P<0.0001. AgNPs, silver nanoparticles.

acid, hymenialdisine, keramaphidin B, manzacidine A and methoxyhexadecanoic acid) with the kinase domains of EGFR and TrkA, which have been previously revealed to be overexpressed in different cancer cells such as A549, HT-29, MCF7 and PANC-1 (63-68). The binding energies, specific amino acid interactions, presence of ionic bonds, hydrogen bonds and halogens were analyzed (Table III; Figs. 11 and 12).

All compounds except keramaphidin B formed hydrogen bonds with key amino acid residues such as Leu718, Lys745 or Met793 within EGFR. The results indicated that keramaphidin B had the most favorable binding energy (-7.15 kcal/mol), followed by debromohymenialdisine (-6.68 kcal/mol) and hymenialdisine (-6.65 kcal/mol). Dacomitinib, the control compound, indicated a binding energy of -7.48 kcal/mol and

Table I. Analysis of the *Stylissa carteri* extract components using liquid chromatography-mass spectrometry.

Compound name	Molecular formula	M/Z	Composition (%)
Calthramide	$C_2H_{15}BrN_4O_3$	343.10	11.0
Agelongine	$C_{13}H_{11}BrN_2O_4$	339.10	9.6
Manzacidine A	$C_{12}H_{14}BrN_3O_4$	344.16	13.0
Debromohymenialdisine	$C_{11}H_{11}N_5O_2$	245.20	12.5
Spongiacidine	$C_{11}H_{11}Br_2N_5O_2$	405.05	10.5
Hymenialdisine	$C_{11}H_{10}BrN_5O_2$	324.13	17.8
3-Bromohymenialdisine	$C_{11}H_9Br_2N_5O_2$	403.03	9.1
Ageliferin	$C_{22}H_{24}Br_2N_{10}O_2$	620.30	9.5

M/Z, mass-to-charge ratio.

Table II. Analysis of the *Amphimedon chloros* extract components using liquid chromatography-mass spectrometry.

Compound name	Molecular formula	M/Z	Composition (%)
Tricosenal	$C_{23}H_{44}O$	336.6	6.4
Tricosenoic acid	$C_{23}H_{44}O_2$	352.6	4.1
Pentacosenal	$C_{25}H_{48}O$	364.6	3.5
Pentacosenic acid	$C_{25}H_{48}O_3$	396.6	3.2
Methoxyhexadecanoic acid	$C_{18}H_{36}O_3$	300.5	9.1
Hydroxytricosanoic acid	$C_{23}H_{46}O_3$	370.6	11.4
Zamamidine	$C_{49}H_{60}N_6O$	749.0	5.1
Keramamine	$C_{23}H_{33}N_3$	380.0	8.7
Ircinol	$C_{26}H_{40}N_2O_2$	412.6	6.4
Keramaphidin B	$C_{26}H_{40}N_2$	351.5	10.2
Purine	$C_5H_4N_4$	120.1	7.1
Pyrinodemin	$C_{37}H_{57}N_3O$	559.9	8.9
Nakinadine	$C_{27}H_{40}N_2O_2$	424.6	8.1
Hachijodine	$C_{19}H_{34}N_2O$	306.5	3.4

M/Z, mass-to-charge ratio.

formed hydrogen bonds with Thr790 and Met793. However, it lacked several interactions observed in the marine compounds, such as interactions with Leu718 and Lys745.

Furthermore, keramaphidin B also demonstrated the strongest binding affinity (-7.08 kcal/mol), followed by hymenialdisine (-6.95 kcal/mol) and debromohymenialdisine (-6.71 kcal/mol), against TrkA. Similar to EGFR, all compounds except keramaphidin B formed hydrogen bonds with residues such as Leu516 and Val524.

The findings suggested that several marine compounds, particularly hymenialdisine and debromohymenialdisine, may potentially interact with and inhibit both EGFR and TrkA. These results indicated that these compounds interact with specific residues (Leu718 and Lys745 in EGFR; Leu516 and Val524 in TrkA), which was not observed with the control compounds. Therefore, this may indicate a unique binding mode.

Co-administering sponge extracts with AgNPs enhances the antibacterial activity. Sponge ethyl acetate extracts combined with AgNPs were tested against six bacterial species using the disc diffusion method (Table IV). In addition, 20 μg/disc AgNPs or sponge ethyl acetate extract alone was administered. The AgNPs and sponge ethyl acetate extract were combined in proportions of 5 or 10 μg/disc of AgNPs with 10 μg/disc of ethyl acetate extract for synergistic tests. Using 20 μg/disc AgNPs alone resulted in ~10 mm-diameter inhibition zones against the majority of bacteria, except for *Enterobacter aerogenes*, which had an increased susceptibility and an inhibition zone of 28.33 mm. All bacterial species, with inhibition zone diameters ranging from 21.43-13.58 mm, were suppressed by the 20 μg/disc *Stylissa carteri* ethyl acetate extract. However, the 20 μg/disc *Amphimedon chloros* extract had no effect on *Enterobacter aerogenes* or *Klebsiella oxytoca*, and the remaining bacterial species had inhibition zones that ranged in diameter from 7.34-15.15 mm. When using the extracts alone, the *Stylissa carteri* extract had an increased inhibitory effect against the six investigated bacterial species compared with the *Amphimedon chloros* extract. Additionally, when

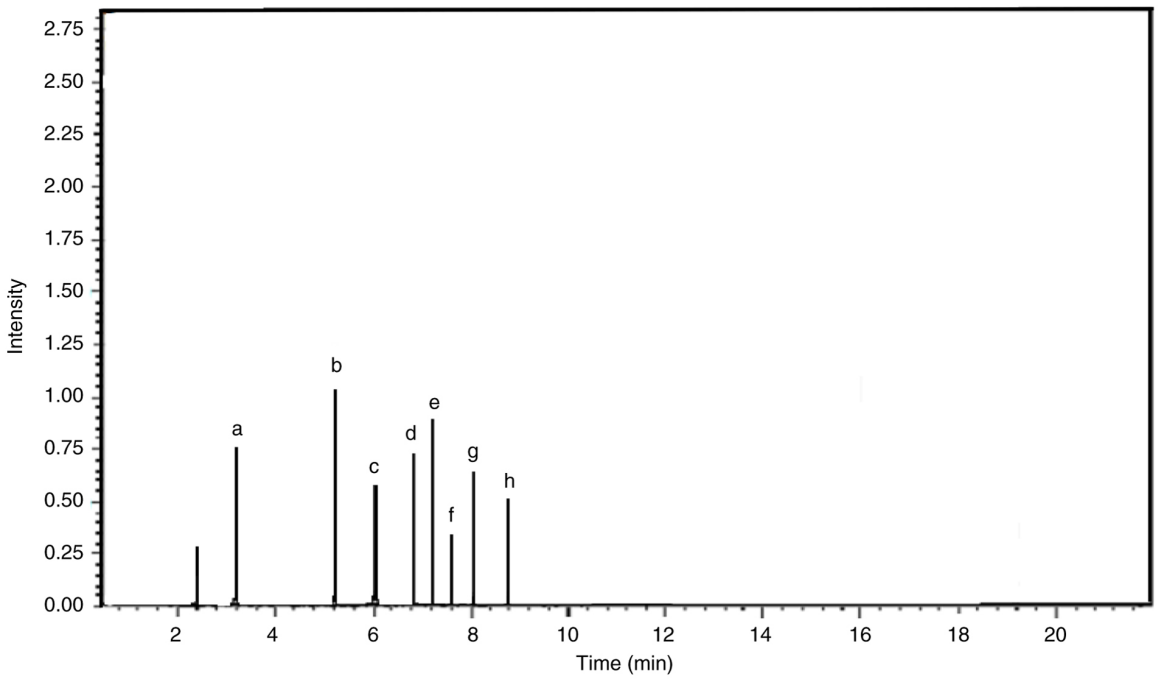

Figure 8. Liquid chromatography-mass spectrometry chromatogram of the components in the *Stylissa carteri* extract. Chromatogram of the *Stylissa carteri* extract with peaks that correspond to individual compounds, which were identified based on their mass-to-charge ratio. Each peak provided detail on the chemical composition of the extract and the relative abundance of its components. The chromatogram revealed the molecular profile of *Stylissa carteri* and highlighted key compounds such as (a) debromohymenialdisine, (b) hymenialdisine, (c) agelongine, (d) calthramide, (e) manzacidine A, (f) 3-bromohymenialdisine, (g) spongiacidine and (h) ageliferin. The chromatogram corresponds to ions with an m/z of 193.00, which have a relative intensity of 81.82% compared with the total ion intensity across all detected m/z values. The maximum intensity range or full-scale limit of the detector was 1,000,000,000. m/z, mass-to-charge ratio.

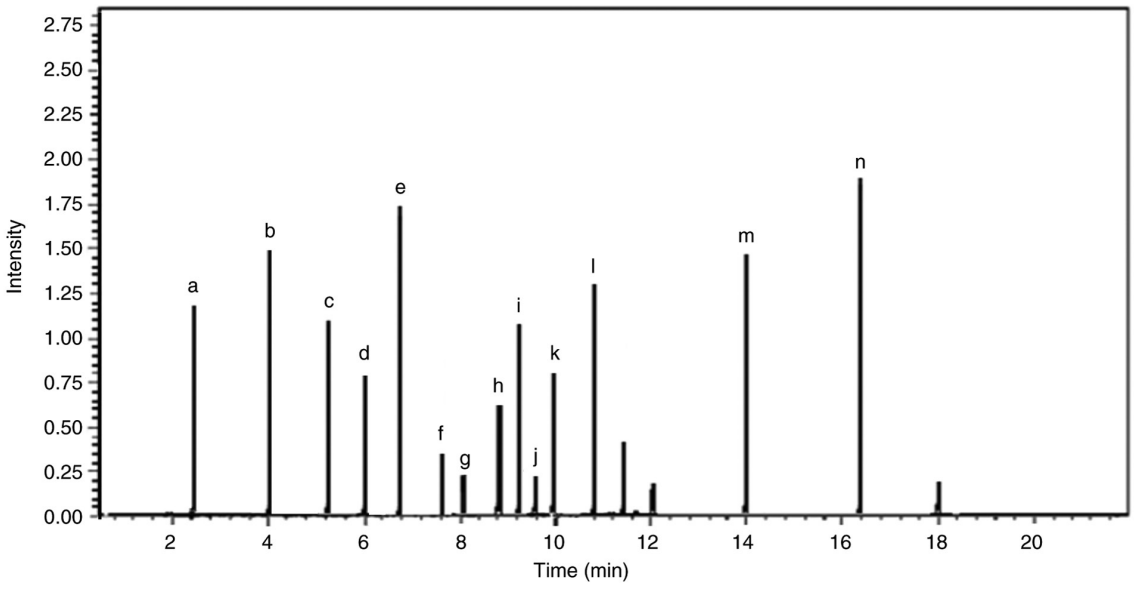

Figure 9. Liquid chromatography-mass spectrometry chromatogram of the components in the *Amphimedon chloros* extract. Chromatogram of the *Amphimedon chloros* extract with peaks that correspond to individual compounds, which were identified based on their mass-to-charge ratio. Each peak provided detail on the chemical composition of the extract and the relative abundance of its components. The chromatogram revealed the molecular profile of *Amphimedon chloros* and highlighted key compounds such as (a) purine, (b) methoxyhexadecanoic acid, (c) hachijodine, (d) tricosenal, (e) kermaphidine B, (f) tricosenoic acid, (g) pentacosenal, (h) zamamidine, (i) karamamine, (j) pentacosenic acid, (k) ircinol, (l) pyrinodemin, (m) nakinadine and (n) hydroxytricosanoic acid. The chromatogram corresponds to ions with an m/z of 193.00, which have a relative intensity of 81.82% compared with the total ion intensity across all detected m/z values. The maximum intensity range or full-scale limit of the detector was 1,000,000,000. m/z, mass-to-charge ratio.

combining 10 μg/disc sponge extract with 5 or 10 μg/disc AgNPs, the majority of the bacterial species investigated had increased inhibition zones and increased fold area (IFA) values when using the *Stylissa carteri* extract compared with the *Amphimedon chloros* extract, except for *E. coli* in which the opposite results were demonstrated. The results indicated that

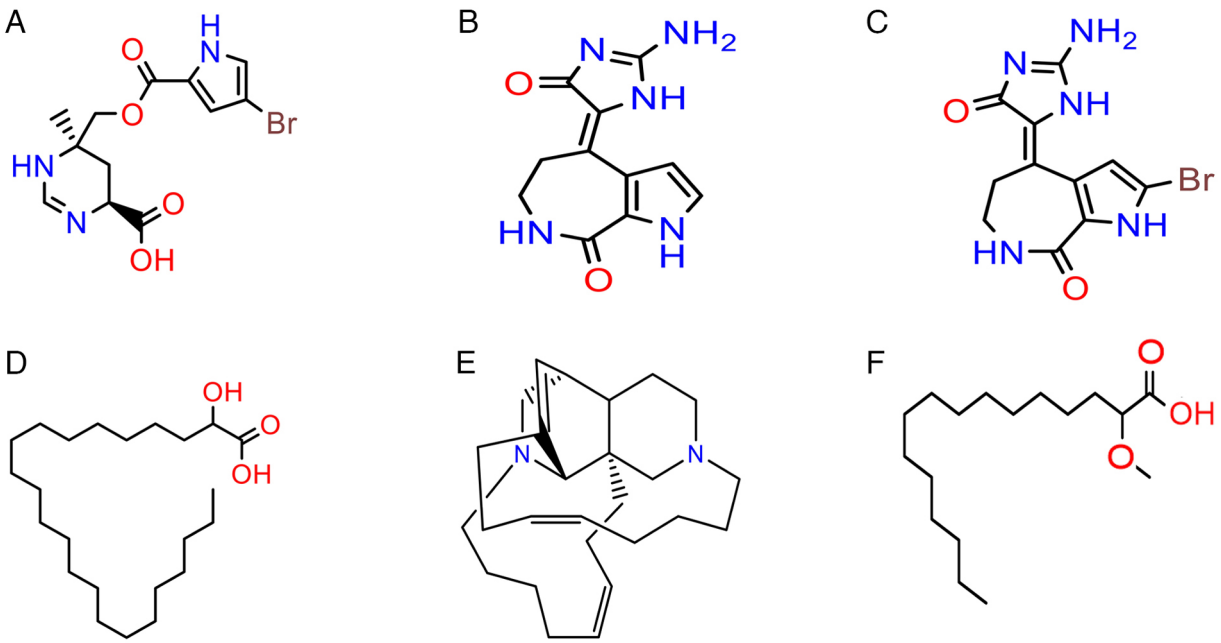

Figure 10. Chemical structures of the main components in the *Stylissa carteri* and *Amphimedon chloros* extracts. (A) Manzacidine A, (B) debromohymenialdisine and (C) hymenialdisine were the main components in the *Stylissa carteri* extract. (D) Hydroxytricosanoic acid, (E) kermaphidine B and (F) methoxyhexadecanoic acid were the main components in the *Amphimedon chloros* extract.

the bacterial species exhibited different responses, which were caused either by the combined treatment of AgNPs with the sponge extract or by the effect of each treatment alone. These results suggest the possibility of using AgNPs in combination with a sponge ethyl acetate extract to treat bacterial infections in hydatid cysts.

Discussion

To the best of our knowledge, the present study was the first to investigate the combined effects of AgNPs with the extracts of two sponge species, *Stylissa carteri* and *Amphimedon chloros*, in order to evaluate their potential as antibacterial and anticancer agents. In the present study, four cancer cell lines (namely A549, PANC-1, HT-29 and MCF7 from lung, pancreatic, colorectal and breast cancer, respectively). These cancer types were selected due to their notable incidence rates, and across all types of cancer diagnoses globally, have incidence rates of 18.4% for lung cancer, 13.1% for breast cancer, 9.7% for pancreatic cancer and 11.2% for colorectal (colon) cancer. In terms of the global cancer-related mortality rates, lung cancer accounts for 32.8% of mortalities, followed by pancreatic and colorectal cancers at 7.4% each, and breast cancer at 4.0% (2,69). Furthermore, these tumors frequently have non-specific symptoms such as, fatigue, weight loss, pain and gastrointestinal disorders, which can interfere with the correct diagnosis as these symptoms are observed in a number of different types of cancer (69,70). In addition, they have genetic and epigenetic changes, such as mutations in the Myc and Ras oncogenes, which are considered notable targets for developing treatments (71-73). Treatment of these types of cancer cells is made more difficult by their metastatic propensity, which requires an alternative treatment approach (74). Therefore, investigating these cell lines is necessary in order to develop treatment approaches and reduce their impact on public health (75,76).

To investigate the anticancer activities of the *Amphimedon chloros* and *Stylissa carteri* marine sponge extracts, the cytotoxic effects were investigated using the extracts separately and in combination with AgNPs. Various cancer cell lines were used including A549, HT-29, MCF7 and PANC-1, as well as the HUVEC normal cell line. To investigate the antibacterial activity of the *Amphimedon chloros* and *Stylissa carteri* extracts alone or with AgNPs, pathogenic bacteria were used, which were isolated from hydatid cyst fluid from damaged anatomical sites including the lung and liver (55). Several previous studies investigate the anticancer and antimicrobial properties of naturally occurring AgNPs derived from fungal origins (77-86).

The present study used LC-MS analysis, which revealed the main active chemical components in both sponge species, and molecular docking, which indicated the potential processes that may underlie their bioactivity. Cytotoxicity was observed when *Amphimedon chloros* or *Stylissa carteri* were combined with AgNPs and applied to different cancer cell lines. However, the impact of AgNPs in combination with *Stylissa carteri* was only significant in the A549 cell line. This synergistic effect may be explained by the presence of the bioactive chemicals present in the sponge extract, which may have increased the efficiency of the AgNPs by facilitating their contact with or absorption by the cancer cells. The LC-MS experiment indicated that *Amphimedon chloros* and *Stylissa carteri* had different chemical components, which may be the reason for the differences in their synergistic effects. Substances such as debromohymenialdisine, hymenialdisine and keramaphidin B may act in combination with AgNPs to inhibit the growth of cancer cells (87-92). Recently, certain sponge components, such as stylissamide, 6-bromotrisindoline,

Table III. Binding interactions and affinity analysis of the selected marine components against the EGFR kinase domain and TrkA after molecular docking.

A, EGFR kinase domain

Compound	LEB (kcal/mol)	Interacting amino acid per interaction type			
		Ionic	H-bond	Halogen	Other binding residues
Debromohymenialdisine	-6.68	None	Gln791, Met793, Arg841, Asn842 and Asp855	None	Leu 718, Ala 743, Lys 745, Thr 790, Leu792, Gly 796, Cys 797 and Thr 854
Hydroxytricosanoic acid	-3.77	None	Glu762 and Thr854	None	Leu718, Val726, Ala743, Lys 745, Met 766, Leu 788, Thr 790, Gln 791, Leu 792, Met 793,Pro 794, Gly 796, Cys 797,Arg 841,Asn 842, Leu 844 , Asp 855 and Phe 856
Hymenialdisine	-6.65	None	Met 793, Arg 841, Asn 842 and Asp 855	None	Leu 718, Val 726, Ala 743, Lys 745, Thr 790, Gln791, Leu 792, Gly 796, Cys797, Leu 844 and Thr 854
Keramaphidin B	-7.15	None	None	None	Leu 718, Gly719, Ser 720, Val 726, Ala 743, Lys 745, Thr 790, Leu 792, Met 793, Gly 796, Cys 797, Asp 800, Arg 841, Leu 844, Thr 854 and Asp 855
Manzacidine A	-6.16	Asp 855	Glu 762 and Met 793	None	Leu 718, Val 726, Ala 743, Thr 754, Met 766, Cys 775, Leu 788, Thr 790, Leu 792, Pro 794, Gly 796 and Leu 844
Methoxyhexadecanoic acid	-4.62	None	Met 793	None	Leu 718, Val 726, Ala 743, Ile 744, Lys 745, Glu762, Met 766, Leu788, Thr790, Gln 791, Leu792, Gly796, Leu 844, Thr 854 and Asp 855
Dacomitinib (control)	-7.48	None	Thr 790 and Met 793	Glu 762	Leu718, Val726, Ala743, Lys745, Met766, Leu788, Gln791, Leu792, Pro794, Gly 796 ,Cys 797, Leu 844), Thr 854 and Asp 855
Repotrectinib (control)	-	-	-	-	-

B, TrkA

Compound	LEB (kcal/mol)	Interacting amino acid per interaction type			
		Ionic	H-bond	Halogen	Other binding residues
Debromohymenialdisine	-6.71	None	Glu 590, Met 592 and Asp 668	None	Leu 516, Val 524, Ala542, Lys 544, Val 573, Phe 589, Tyr 591, Gly 595, Leu 657, Gly 667 and Arg 673
Hydroxytricosanoic acid	-4.60	None	Asp 596 and Arg 673	None	Leu 516, Gly 517, Val 524, Ala 542, Lys 544, Val 573, Phe 589, Gly 595, Arg 599, Arg 654, Asn 655 , Cys 656, Leu 657, Gly 667 and Asp 668
Hymenialdisine	-6.95	None	Glu 590, Met 592 and Asp 668	None	Leu 516, Val 524, Ala 542, Lys 544, Val 573, Phe 589, Tyr 591, Gly 595, Asp 596, Leu 657, Gly 667 and Arg 673
Keramaphidin B	-7.08	None	None	None	Leu 516, Gly 517, Glu 518, Val 524, Lys 544, Asp 558, Gly 595, Asp 596, Arg 654, Asn 655, Cys 656, Leu 657, Gly 667 and Arg 673

Table III. Continued.

B, TrkA

Compound	LEB (kcal/mol)	Interacting amino acid per interaction type			
		Ionic	H-bond	Halogen	Other binding residues
Manzacidine A	-6.32	None	Glu 590, Met 592 and Arg 673	None	Leu 516, Gly 517, Val 524, Ala 542, Val 573, Phe 589, Tyr 591, Gly 595, Asp 596, Leu 657 and Gly 667
Methoxyhexadecanoic acid	-4.37	None	Asp 596 and Arg 673	None	Leu 516, Gly 517, Val 524, Ala 542, Lys 544, Val 573, Phe 589, Glu 590, Tyr 591, Met 592, Gly 595 and Leu 657
Dacomitinib (control)	-	-	-	-	-
Repotrectinib (control)	-9.23	None	Met 592 and Gly 667	Asn 655 and Cys 656	Leu 516, Gly 517, Val 524, Ala 542, Lys 544, Val 573, Phe 589, Glu 590, Tyr 591, Gly 595, Asp 596, Arg654, Leu 657, Asp 668 and Arg 673

EGFR, epidermal growth factor receptor; TrkA, tyrosine kinase receptor A; LEB, lowest free energy of binding; H-bond, hydrogen bond.

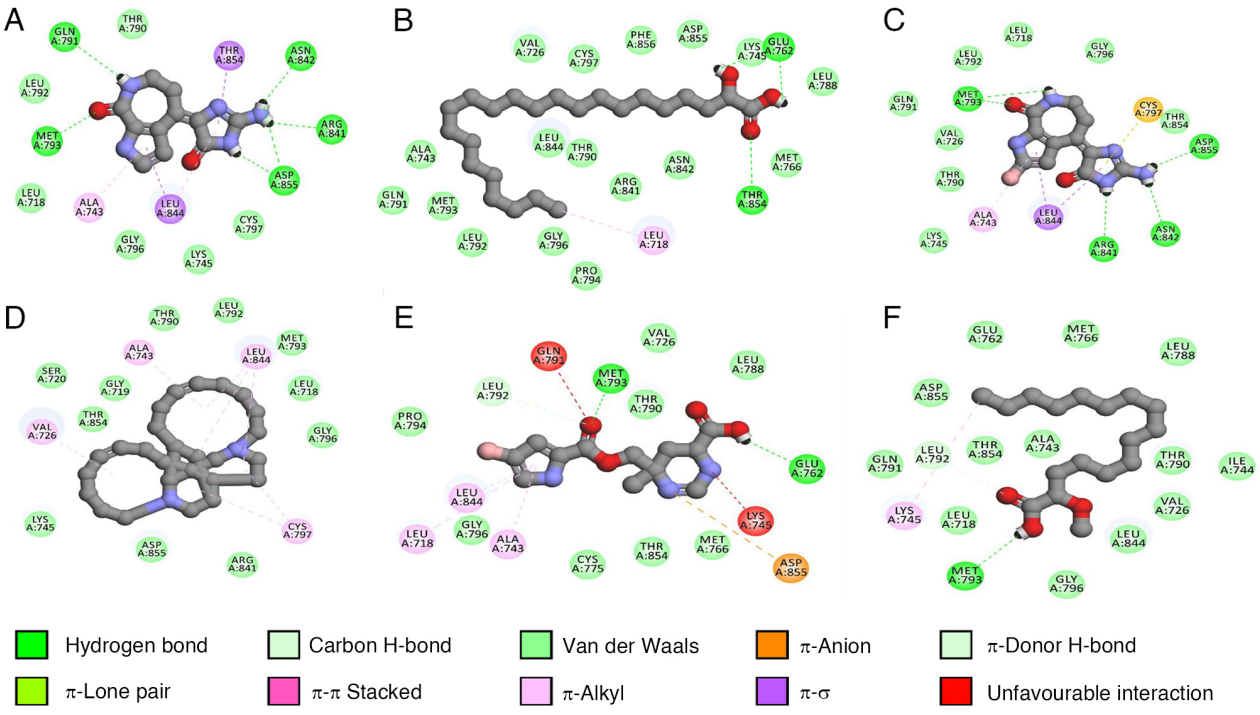

Figure 11. Binding interactions of six marine-derived compounds with the epidermal growth factor receptor. Ball and stick representation of (A) debromohymenialdisine, (B) hydroxytricosanoic acid, (C) hymenialdisine, (D) keramaphidin B, (E) manzacidine A and (F) methoxyhexadecanoic acid docked against the epidermal growth factor receptor kinase domain (Protein Data Bank ID, 4I23; https://www.rcsb.org/structure/4i23). The figure was created using Biovia Discovery Studio Visualiser 2016® (Dassault Systèmes). H-bond, hydrogen bond.

N-(2-hydroxyphenyl)-acetamide, petrocidin A, 2,3-dihydroxybenzamid, 6-bromotrisindoline and geodiataurine, have been revealed to have anti-proliferative capabilities against cancer cells (93,94). Additionally, keramaphidin B, which is known to be an important constituent of *Amphimedon chloros*, has a cytotoxic impact on a number of cancer cell lines, including P388 murine leukemia cells and KB human epidermoid carcinoma cells (89). However, neither the mechanism nor the possible synergistic effects of keramaphidin B in combination with AgNPs have been investigated. Furthermore, hymenialdisine, which is identified as the main component of *Stylissa carteri*, inhibited the growth of ovarian cancer cell lines, and demonstrated an antiangiogenic activity by blocking NF-κB activity and angiogenic factors such as vascular endothelial growth

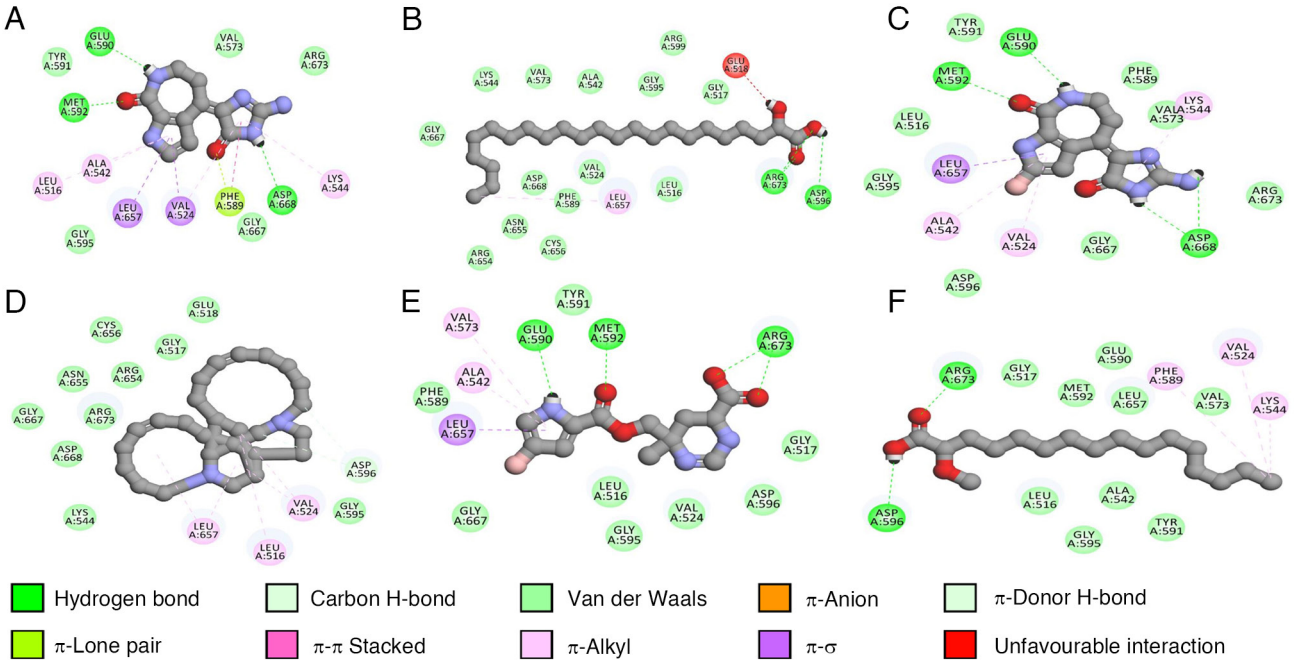

Figure 12. Binding interactions of six marine-derived compounds with the tyrosine kinase receptor A. Ball and stick representation of (A) debromohymenialdisine, (B) hydroxytricosanoic acid, (C) hymenialdisine, (D) keramaphidin B, (E) manzacidine A and (F) methoxyhexadecanoic acid docked against tyrosine kinase receptor A (Protein Data Bank ID, 7VKO; https://www.rcsb.org/structure/7VKO). The figure was created using Biovia Discovery Studio Visualiser 2016® (Dassault Systèmes). H-bond, hydrogen bond.

factor and IL-8 (91,92). Furthermore, debromohymenialdisine, which is also indicated to be a component of *Stylissa carteri*, increases cell cycle arrest by inhibiting the G2 phase in the MCF7 cell line (87).

Due to their function in cancer cell signaling pathways, their overexpression or mutation in a variety of types of cancer (including lung, pancreatic, colorectal and breast cancers) and their potential as therapeutic targets for inhibiting tumor growth and progression, EGFR and TrkA were chosen for docking experiments (95). We hypothesize that the activity of the sponge components (such as debromohymenialdisine, hydroxytricosanoic acid, hymenialdisine, keramaphidin B, manzacidine A and methoxyhexadecanoic acid) originates from the possible interaction of these components with TrkA and EGFR, which in turn may inhibit various pathways that promote the growth of cancer, including the phoshoinositide-3-kinase/Akt and mitogen-activated protein kinase/extracellular signal-regulated kinase signaling pathways. This may accelerate the process of apoptosis, cause cell cycle arrest, oppose the metastatic stage and prevent cancer cells from proliferating. Furthermore, the present study also demonstrated the cytotoxicity of combining the sponge extracts with AgNPs. The combination of 6 µg/ml *Stylissa carteri* extract with 0.75 µg/ml AgNPs revealed a relatively low cytotoxicity in HUVEC cells, with a 25.97% cell cytotoxicity, suggesting minimal toxicity at this dose. However, this cytotoxic effect was not significantly different compared with the *Stylissa carteri* extract alone at the same concentration. By contrast, a significant reduction in the cytotoxicity of the HUVEC cells was revealed when the *Amphimedon chloros* extract was used across concentrations ranging from 6-200 µg/ml in combination with 0.75 µg/ml AgNPs compared with the *Amphimedon chloros* extract alone. This selectivity suggested that the combination of sponge extracts with AgNPs has a possible therapeutic potential as a low cytotoxicity against HUVEC normal cells is an important factor for the development of safer anticancer agents (96). The present study highlighted the potential of analyzing marine products, indicating that they may be used to find new drugs among the vast resources that are present in the water of the Aqaba Gulf and other seas located within the sub-tropical arid climate.

The combination of the *Stylissa carteri* extract with AgNPs demonstrated the strongest synergistic action against *Micrococcus* spp., with an IFA of 3.43. The catalytic reactivity of nanoparticles is primarily dependent on their surface area and increases as the surface energy increases (97). However, AgNPs can have harmful effects (such as DNA damage, inflammation and apoptosis) due to their ability to induce the production of reactive oxygen species (such as hydrogen peroxide and superoxide anions) (57,98). The antibacterial activities of the AgNPs, the sponge ethyl acetate extracts and the AgNPs combined with the sponge ethyl acetate extracts demonstrated inconsistencies between the different treatment groups, regardless of Gram status of the bacteria. Therefore, it was hypothesized that the structural variations of the membranes could not be the reason behind this variation. A number of compounds, such as debromohymenialdisine, hydroxytricosanoic acid, hymenialdisine, keramaphidin B, manzacidine A and methoxyhexadecanoic acid, extracted using ethyl acetate, which is a semi-polar solvent, have a high level of antibacterial activity (99-104). Using the *Stylissa carteri* extract alone produced inhibitory zones in the six bacterial species investigated, and had an increased antibacterial efficacy compared with the extract of *Amphimedon chloros*. Using marine natural components reveals synergistic effects with antimicrobial medicines (99,105). For example, several marine

Table IV. Antibacterial and synergistic effects of *Stylissa carteri* or *Amphimedon chloros* ethyl acetate extracts and AgNPs against bacteria isolated from echinococcal hydatid cyst fluid.

A, *Stylissa carteri*

	Inhibition zones (mm)				
Bacteria	AgNPs (20 μg/disc)	Sponge (20 μg/disc)	AgNPs (5 μg/disc) plus sponge (10 μg/disc)	AgNPs (10 μg/disc) plus sponge (10 μg/disc)	IFA[a]
Staphylococcus xylosus	10.40±0.15	21.43±0.17	16.00±0.12	20.00±0.18	2.70±0.13
Klebsiella oxytoca	10.65±0.14	15.92±0.16	12.77±0.13	16.54±0.19	1.40±0.08
Enterobacter aerogenes	28.33±0.18	13.58±0.15	17.14±0.14	30.79±0.16	0.18±0.02
Micrococcus spp.	9.75±0.13	21.00±0.18	13.60±0.12	20.52±0.17	3.43±0.14
Pseudomonas aeruginosa	9.40±0.16	16.09±0.15	13.38±0.11	14.96±0.13	1.53±0.10
Escherichia coli	10.17±0.14	13.93±0.17	12.44±0.16	16.71±0.18	1.70±0.09

B, *Amphimedon chloros*

	Inhibition zones (mm)				
Bacteria	AgNPs (20 μg/disc)	Sponge (20 μg/disc)	AgNPs (5 μg/disc) plus sponge (10 μg/disc)	AgNPs (10 μg/disc) plus sponge (10 μg/disc)	IFA[a]
Staphylococcus xylosus	10.40±0.13	9.00±0.12	11.19±0.15	13.23±0.14	0.62±0.05
Klebsiella oxytoca	10.65±0.16	0.00±0.00	9.48±0.14	12.28±0.15	0.33±0.03
Enterobacter aerogenes	28.33±0.17	0.00±0.00	8.88±0.12	15.93±0.16	0.00±0.00
Micrococcus spp.	9.75±0.12	8.77±0.13	8.90±0.14	11.99±0.15	0.51±0.05
Pseudomonas aeruginosa	9.40±0.14	15.00±0.16	9.66±0.11	11.39±0.13	0.47±0.06
Escherichia coli	10.17±0.15	7.34±0.12	18.00±0.19	19.71±0.18	2.76±0.13

[a]An IFA of individual AgNPs, which was calculated using $C=(B^2-A^2)/A^2$; where, A and B are the inhibition zones (mm) obtained for 20 μg/disc AgNPs alone and 10 μg/disc AgNPs with 10 μg/disc *Stylissa carteri* or *Amphimedon chloros* ethyl acetate extract, respectively. The results are presented as means ± SD (n=3). AgNPs, silver nanoparticles; IFA, increase in fold area.

sources have produced natural compounds such as equisetin, D-mannose, cis-vaccenic acid, trans-13-octadecenoic acid, stigmasterol and retinoyl-β-glucuronide with antibiotic-resistant microorganism-fighting capabilities (94,106,107). A number of them have stronger antimicrobial activity compared with therapeutic antibacterial/antifungal drugs. For example, an epoxy sponge sterol, 9α,11α-epoxycholest-7-ene-3β,5α,6α,19-tetrol-6 acetate (ECTA) was the first marine natural substance to reverse the multidrug efflux pump-mediated fluconazole resistance of *Candida albicans* (108,109). Combining fluconazole with ECTA (3.8 μM) increases its antifungal efficacy by 35 times (105). Marine sponges are the animal kingdoms that create the largest quantities of bioactive chemicals (110). Currently, it is unclear if the combination of AgNPs and sponge ethyl acetate extracts will be additive or synergistic, as their ability to penetrate the bacterial envelope is still poorly understood.

Although the present study offered insights regarding the potential synergistic effects of AgNPs combined with the ethyl acetate extracts of marine sponges *Amphimedon chloros* or *Stylissa carteri*, a number of limitations should be addressed. Firstly, there was a lack of results on the combined effect of *Stylissa carteri* and *Amphimedon chloros* extracts with and without AgNPs, as well as a lack of an evaluation of these combinations on a control 'normal' human cell line. Additionally, *in vivo* validation is required to investigate the therapeutic potential and safety. Furthermore, the mechanisms proposed in the present study regarding TrkA and EGFR requires further comprehensive mechanistic investigation. Although important chemical components were identified using LC-MS analysis, the entire spectrum of bioactive chemicals was not fully investigated. In addition, the number of cancer cell lines and bacterial strains investigated in the presence of these compounds was limited in the present study. Therefore, the present study was not sufficient in demonstrating the therapeutic prospects of these components for cancer and bacterial infections. However, it provided a framework for future investigations and highlighted the possibility of combining AgNPs with marine sponge extracts as potential options for antibacterial and cancer therapy.

In conclusion, the observed cytotoxic effects of *Amphimedon chloros* and *Stylissa carteri* extracts combined with AgNPs against a variety of cancer cell lines and bacterial

strains suggests that further investigation on the anticancer and antibacterial potential is warranted.

Future studies should focus on elucidating the precise mechanisms of the interaction between the sponge-derived compounds and AgNPs. Furthermore, the combination ratios between the sponge extracts (such as *Stylissa carteri* and *Amphimedon chloros*) and between the sponges extracts and AgNPs should be optimized for the maximum efficacy. Additionally, the therapeutic potential should be evaluated *in vivo*. The results of the present study indicated the importance of marine biodiversity as a source of novel therapeutic agents and highlighted the potential of combining natural products with nanotechnology in order to increase their anticancer and antibacterial properties.

Acknowledgements

Not applicable.

Funding

No funding was received.

Availability of data and materials

The data generated in the present study may be found in Figshare under accession number 26255297 or at the following URL: https://doi.org/10.6084/m9.figshare.26255297.

Authors' contributions

MA, KK, AAl-S, DA, YQ and AAls participated in the conception and design of the study. Material preparation and analysis were carried out by MA, KK, AAl-S, DA and AF. The docking experiment was carried out by BA and FS. The manuscript was written by MA, YQ and AAls. All authors read and approved the final version of the manuscript. MA and KK confirm the authenticity of all the raw data.

Ethics approval and consent to participate

Not applicable.

Patient consent for publication

Not applicable.

Competing interests

The authors declare that they have no competing interests.

References

1. Gerstberger S, Jiang Q and Ganesh KJC: Metastasis. Cell 186: 1564-1579, 2023.
2. Siegel RL, Miller KD, Wagle NS and Jemal A: Cancer statistics, CA Cancer J Clin 73: 17-48, 2023.
3. Bazeed AY, Day CM and Garg SJC: Pancreatic cancer: Challenges and opportunities in locoregional therapies. Cancers (Basel) 14: 4257, 2022.
4. Vasan N, Baselga J and Hyman DM: A view on drug resistance in cancer. Nature 575: 299-309, 2019.
5. Hossain CM, Gera M and Ali KA: Current status and challenges of herbal drug development and regulatory aspect: A global perspective. Asian J Pharmaceutical Clin Res 15: 31-41, 2022.
6. Abdussalam-Mohammed W: Review of therapeutic applications of nanotechnology in medicine field and its side effects. J Chem Rev 1: 243-251, 2019.
7. Nirmala MJ, Kizhuveetil U, Johnson A, Balaji G, Nagarajan R and Muthuvijayan V: Cancer nanomedicine: A review of nano-therapeutics and challenges ahead. RSC Adv 13: 8606-8629, 2023.
8. Bhattacharjee S: Craft of co-encapsulation in nanomedicine: A struggle to achieve synergy through reciprocity. ACS Pharmacol Transl Sci 5: 278-298, 2022.
9. Fan H, Sun Q, Dukenbayev K, Benassi E, Manarbek L, Nurkesh AA, Khamijan M, Mu C, Li C, Razbekova M, *et al*: Carbon nanoparticles induce DNA repair and PARP inhibitor resistance associated with nanozyme activity in cancer cells. Res Square 13: 39, 2022.
10. Elmehrath S, Nguyen HL, Karam SM, Amin A and Greish YE: BioMOF-based anti-cancer drug delivery systems. Nanomaterials 13: 953, 2023.
11. El-kharrag R, Abdel Halim SS, Amin A, Greish YE and Biomaterials P: Synthesis and characterization of chitosan-coated magnetite nanoparticles using a modified wet method for drug delivery applications. Int J Polymeric Materials Polymeric Biomaterials 68: 73-82, 2019.
12. Ibrahim S, Baig B, Hisaindee S, Darwish H, Abdel-Ghany A, El-Maghraby H, Amin A and Greish Y: Development and evaluation of crocetin-functionalized pegylated magnetite nanoparticles for hepatocellular carcinoma. Molecules 28: 2882, 2023.
13. Shaimoldina A, Sergazina A, Myrzagali S, Nazarbek G, Omarova Z, Mirza O, Fan H, Amin A, Zhou W and Xie Y: Carbon nanoparticles neutralize carbon dioxide (CO2) in cytotoxicity: Potent carbon emission induced resistance to anticancer nanomedicine and antibiotics. Ecotoxicol Environ Saf 273: 116024, 2024.
14. El-Kharrag R, Amin A and Greish YEJCI: Low temperature synthesis of monolithic mesoporous magnetite nanoparticles. Ceramics Int 38: 627-634, 2012.
15. Benassi E, Fan H, Sun Q, Dukenbayev K, Wang Q, Shaimoldina A, Tassanbiyeva A, Nurtay L, Nurkesh A, Kutzhanova A and Mu C: Generation of particle assemblies mimicking enzymatic activity by processing of herbal food: The case of rhizoma polygonati and other natural ingredients in traditional Chinese medicine. Nanoscale Adv 3: 2222-2235, 2021.
16. Nazarbek G, Kutzhanova A, Nurtay L, Mu C, Kazybay B, Li X, Ma C, Amin A and Xie Y: Nano-evolution and protein-based enzymatic evolution predicts novel types of natural product nanozymes of traditional Chinese medicine: Cases of herbzymes of Taishan-Huangjing (*Rhizoma polygonati*) and Goji (*Lycium chinense*). Nanoscale Adv 3: 6728-6738, 2021.
17. Xie Y, Shaimoldina A, Fan H, Myrzagali S, Nazarbek G, Myrzagalieva A, Orassay A, Amin A and Benassi E: Characterisation of a phosphatase-like nanozyme developed by baking cysteine and its application in reviving mung bean sprouts damaged by ash. Environ. Sci.: Nano 11: 266-277, 2024.
18. Paiva L, Fidalgo T, Da Costa L, Maia LC, Balan L, Anselme K, Ploux L and Thiré RMSM: Antibacterial properties and compressive strength of new one-step preparation silver nanoparticles in glass ionomer cements (NanoAg-GIC). J Dent 69: 102-109, 2018.
19. Huy TQ, Thanh NTH, Thuy NT, Chung PV, Hung PN, Le AT and Hong Hanh NT: Cytotoxicity and antiviral activity of electrochemical-synthesized silver nanoparticles against poliovirus. J Virol Methods 241: 52-57, 2017.
20. Pawar A, Korde SK, Rakshe DS, William P, Jawale M and Deshpande N: Analysis of Silver Nanoparticles as Carriers of Drug Delivery System. J Nano-Electron Phys 15: 04015, 2023.
21. Naseer F, Ahmed M, Majid A, Kamal W and Phull AR: Green nanoparticles as multifunctional nanomedicines: Insights into anti-inflammatory effects, growth signaling and apoptosis mechanism in cancer. Semin Cancer Biol 86: 310-324, 2022.
22. Sharma P, Hasan MR, Khanuja M, Rawal R, Shivani, Pilloton R and Narang J: Aptamer-based silver nanoparticle decorated paper platform for electrochemical detection ovarian cancer biomarker PDGF. Materials Chemistry Physics 306: 128114, 2023.
23. Zhang Y, Han X, Liu Y, Wang S, Han X and Cheng C: Research progress on nano-sensitizers for enhancing the effects of radiotherapy. Materials Adv 3: 3709-3725, 2022.

24. Kitic D, Miladinovic B, Randjelovic M, Szopa A, Seidel V, Prasher P, Sharma M, Fatima R, Arslan Ateşşahin D, Calina D and Sharifi-Rad J: Anticancer and chemopreventive potential of *Morinda citrifolia* L. bioactive compounds: A comprehensive update. Phytother Res 38: 1932-1950, 2024.
25. Minhas LA, Kaleem M, Farooqi HMU, Kausar F, Waqar R, Bhatti T, Aziz S, Jung DW and Mumtaz AS: Algae-derived bioactive compounds as potential nutraceuticals for cancer therapy: A comprehensive review. Algal Res 78: 103396, 2024.
26. Al-Hrout A, Baig B, Hilal-Alnaqbi A and Amin A: Cancer and biotechnology: A matchup that should never slowdown. In: Biotechnology and Production of Anti-Cancer Compounds, Springer International, (pp.73-97), 2017.
27. Sahoo A, Mandal AK, Kumar M, Dwivedi K and Singh D: Prospective challenges for patenting and clinical trials of anti-cancer compounds from natural products: Coherent review. Recent Pat Anticancer Drug Discov 18: 470-494, 2023.
28. Amin A and Buratovich M: The anti-cancer charm of flavonoids: A cup-of-tea will do! Recent Pat Anticancer Drug Discov 2: 109-117, 2007.
29. Xie Y, Mu C, Kazybay B, Sun Q, Kutzhanova A, Nazarbek G, Xu N, Nurtay L, Wang Q, Amin A and Li X: Network pharmacology and experimental investigation of *Rhizoma polygonati* extract targeted kinase with herbzyme activity for potent drug delivery. Drug Deliv 28: 2187-2197, 2021.
30. Badran MM, Alouny NN, Aldosari BN, Alhusaini AM and Abou El Ela AES: Transdermal glipizide delivery system based on chitosan-coated deformable liposomes: development, ex vivo, and in vivo studies. Pharmaceutics 14: 826, 2022.
31. Murali C, Mudgil P, Gan CY, Tarazi H, El-Awady R, Abdalla Y, Amin A and Maqsood S: Camel whey protein hydrolysates induced G2/M cellcycle arrest in human colorectal carcinoma. Sci Rep 11: 7062, 2021.
32. Mathew BT, Torky Y, Amin A, Mourad AI, Ayyash MM, El-Keblawy A, Hilal-Alnaqbi A, AbuQamar SF and El-Tarabily KA: Halotolerant marine rhizosphere-competent actinobacteria promote *Salicornia bigelovii* growth and seed production using seawater irrigation. Front Microbiol 11: 552, 2020.
33. Ortigosa-Palomo A, Quiñonero F, Ortiz R, Sarabia F, Prados J and Melguizo C: Natural products derived from marine sponges with antitumor potential against lung cancer: A systematic review. Mar Drugs 22: 101, 2024.
34. Shady NH, Fouad MA, Salah Kamel M, Schirmeister T and Abdelmohsen UR: Natural product repertoire of the genus Amphimedon. Mar Drugs 17: 19, 2018.
35. Hardani IN, Damara FA, Nugrahani AD and Bashari MH: Ethanol extract of *Stylissa carteri* induces cell death in parental and paclitaxel-resistant cervical cancer cells. IJIHS 6: 91-96, 2018.
36. Al-Soub A, Khleifat K, Al-Tarawneh A, Al-Limoun M, Alfarrayeh I, Sarayreh AA, Qaisi YA, Qaralleh H, Alqaraleh M and Albashaireh A: Silver nanoparticles biosynthesis using an airborne fungal isolate, *Aspergillus flavus*: Optimization, characterization and antibacterial activity. Iran J Microbiol 14: 518-528, 2022.
37. Jaidev L and Narasimha G: Fungal mediated biosynthesis of silver nanoparticles, characterization and antimicrobial activity. Colloids Surf B Biointerfaces 81: 430-433, 2010.
38. Hooper JN and Van Soest RW: Systema Porifera. A guide to the classification of sponges. In: Systema Porifera: A guide to the classification of sponges. Springer, ppl-7, 2002.
39. Helmy T and Van Soest R: Amphimedon species (Porifera: Niphatidae) from the Gulf of Aqaba, Northern Red Sea: Filling the gaps in the distribution of a common pantropical genus. Zootaxa 859: 1, 2005.
40. O'Rourke A, Kremb S, Duggan BM, Sioud S, Kharbatia N, Raji M, Emwas AH, Gerwick WH and Voolstra CR: Identification of a 3-alkylpyridinium compound from the red sea sponge *Amphimedon chloros* with in vitro inhibitory activity against the West Nile Virus NS3 protease. Molecules 23: 1472, 2018.
41. Bashari MH, Huda F, Tartila TS, Shabrina S, Putri T, Qomarilla N, Atmaja H, Subhan B, Sudji IR and Meiyanto E: Bioactive compounds in the ethanol extract of marine sponge *Stylissa carteri* demonstrates potential anti-cancer activity in breast cancer cells. Asian Pac J Cancer Prev 20: 1199-1206, 2019.
42. Kandler NM, Wooster MK, Leray M, Knowlton N, de Voogd NJ, Paulay G and Berumen ML: Hyperdiverse macrofauna communities associated with a common sponge, *Stylissa carteri*, shift across ecological gradients in the Central Red Sea. Diversity 11: 18, 2019.
43. Ebada SS, Edrada RA, Lin W and Proksch P: Methods for isolation, purification and structural elucidation of bioactive secondary metabolites from marine invertebrates. Nat Protoc 3: 1820-1831, 2008.
44. Bayona LM, Videnova M and Choi YH: Increasing metabolic diversity in marine sponges extracts by controlling extraction parameters. Mar Drugs 16: 393, 2018.
45. Al-Tawarah NM, Qaralleh H, Khlaifat AM, Nebih Nofal M, Khleifat KM, Al-Limoun MO, Alqaraleh M and Ahmed Al Shhab M: Anticancer and antibacterial properties of verthemia iphionides essential oil/silver nanoparticles. Biomed Pharmacol J 13: 1175-1185, 2020.
46. Alqaraleh M, Khleifat KM, Abu Hajleh MN, Farah HS and Ahmed KAA: Fungal-mediated silver nanoparticle and biochar synergy against colorectal cancer cells and pathogenic bacteria. Antibiotics (Basel) 12: 597, 2023.
47. Nikalje APG and Gadikar R: A simple liquid chromatographic method for simultaneous determination of aceclofenac, methyl salicylate, and benzyl alcohol in pharmaceuticals. J Pharmacy Res 12: 283, 2018.
48. Murray BW, Rogers E, Zhai D, Deng W, Chen X, Sprengeler PA, Zhang X, Graber A, Reich SH, Stopatschinskaja S, *et al*: Molecular characteristics of repotrectinib that enable potent inhibition of TRK fusion proteins and resistant mutations. Mol Cancer Ther 20: 2446-2456, 2021.
49. Gajiwala KS, Feng J, Ferre R, Ryan K, Brodsky O, Weinrich S, Kath JC and Stewart A: Insights into the aberrant activity of mutant EGFR kinase domain and drug recognition. Structure 21: 209-219, 2013.
50. Morris GM, Huey R, Lindstrom W, Sanner MF, Belew RK, Goodsell DS and Olson AJ: AutoDock4 and AutoDockTools4: Automated docking with selective receptor flexibility. J Comput Chem 30: 2785-2791, 2009.
51. Bouabdallah S, Brinza I, Boiangiu RS, Ibrahim MH, Honceriu I, Al-Maktoum A, Cioanca O, Hancianu M, Amin A, Ben-Attia M and Hritcu L: The effect of a Tribulus-based formulation in alleviating cholinergic system impairment and scopolamine-induced memory loss in zebrafish (*Danio rerio*): Insights from molecular docking and in vitro/in vivo approaches. Pharmaceuticals (Basel) 17: 200, 2024.
52. Saqallah FG, Hamed WM, Talib WH, Dianita R and Wahab HA: Antimicrobial activity and molecular docking screening of bioactive components of *Antirrhinum majus* (snapdragon) aerial parts. Heliyon 8: e10391, 2022.
53. Shtaiwi M, Alemleh M, Abu-Safieh KA, Salameha BA, Shtaiwi A, Alwahsh M, Hamadneh L and Khanfar MA: Design, synthesis, crystal structure, biological activity and molecular modeling of novel schiff bases derived from chalcones and 5-Hydrazino-1,3-Dimethyl-4-Nitropyrazole as anticancer agents. Polycyclic Aromatic Compounds 44: 4178-4196, 2023.
54. Biovia: Discovery Studio Modeling Environment. Dassault-Systèmes, San Diego, CA, 2016.
55. Al Qaisi YT, Khleifat KM, Oran SA, Al Tarawneh AA, Qaralleh H, Al-Qaisi TS and Farah HS: Ruta graveolens, Peganum harmala, and Citrullus colocynthis methanolic extracts have in vitro protoscolocidal effects and act against bacteria isolated from echinococcal hydatid cyst fluid. Arch Microbiol 204: 228, 2022.
56. Clinical and Laboratory Standards Institute (CLSI): Performance standards for antimicrobial susceptibility testing. CLSI, Wayne, PA, 2011.
57. Qaralleh H, Khleifat K, Al-Limoun M, Al-Tarawneh A, Khleifat W, Almajali L, Buqain R, Shadid KA and Aslowayeh N: Antibacterial activity of airborne fungal mediated nanoparticles in combination with Foeniculum vulgare essential oil. J Herbmed Pharmacol 11: 419-427, 2022.
58. Amirjani A, Firouzi F and Haghshenas DF: Predicting the size of silver nanoparticles from their optical properties. J Plasmonics 15: 1077-1082, 2020.
59. Abbas R, Luo J, Qi X, Naz A, Khan IA, Liu H, Yu S and Wei J: Silver nanoparticles: Synthesis, structure, properties and applications. Nanomaterials (Basel) 14: 1425, 2024.
60. Al-Samydai A, Abu Hajleh MN, Al-Sahlawi F, Nsairat H, Khatib AA, Alqaraleh M and Ibrahim AK: Advancements of metallic nanoparticles: A promising frontier in cancer treatment. Sci Prog 107: 368504241274967, 2024.
61. Leary M, Heerboth S, Lapinska K and Sarkar S: Sensitization of drug resistant cancer cells: A matter of combination therapy. Cancers 10: 483, 2018.
62. Chenthamara D, Subramaniam S, Ramakrishnan SG, Krishnaswamy S, Essa MM, Lin FH and Qoronfleh MW: Therapeutic efficacy of nanoparticles and routes of administration. Biomater Res 23: 20, 2019.

63. Brunetto de Farias C, Rosemberg DB, Heinen TE, Koehler-Santos P, Abujamra AL, Kapczinski F, Brunetto AL, Ashton-Prolla P, Meurer L, Reis Bogo M, *et al*: BDNF/TrkB content and interaction with gastrin-releasing peptide receptor blockade in colorectal cancer. Oncology 79: 430-439, 2011.
64. Seo JH, Jung KH, Son MK, Yan HH, Ryu YL, Kim J, Lee JK, Hong S and Hong SS: Anti-cancer effect of HS-345, a new tropomyosin-related kinase A inhibitor, on human pancreatic cancer. Cancer Lett 338: 271-281, 2013.
65. Chen B, Liang Y, He Z, An Y, Zhao W and Wu J: Autocrine activity of BDNF induced by the STAT3 signaling pathway causes prolonged TrkB activation and promotes human non-small-cell lung cancer proliferation. Sci Rep 6: 30404, 2016.
66. Kyker-Snowman K, Hughes RM, Yankaskas CL, Cravero K, Karthikeyan S, Button B, Waters I, Rosen DM, Dennison L, Hunter N, *et al*: TrkA overexpression in non-tumorigenic human breast cell lines confers oncogenic and metastatic properties. Breast Cancer Res 179: 631-642, 2020.
67. Griffin N, Marsland M, Roselli S, Oldmeadow C, Attia J, Walker MM, Hondermarck H and Faulkner S: The receptor tyrosine kinase TrkA is increased and targetable in HER2-positive breast cancer. Biomolecules 10: 1329, 2020.
68. Nwaefulu ON, Sagineedu S, Islam MK and Stanslas J: Pancreatic cancer treatment with targeted therapies: Are we there yet? Eur Rev Med Pharmacol Sci 26: 367-381, 2022.
69. Bray F, Laversanne M, Sung H, Ferlay J, Siegel RL, Soerjomataram I and Jemal A: Global cancer statistics 2022: GLOBOCAN estimates of incidence and mortality worldwide for 36 cancers in 185 countries. CA Cancer J Clin 74: 229-263, 2024.
70. de Chiffre JMD, Ormstrup TE, Kusk MW and Hess S: Patients from general practice with non-specific cancer symptoms: A retrospective study of symptoms and imaging. BJGP Open 8: BJGPO.2023.0058, 2024.
71. Park JW and Han JW: Targeting epigenetics for cancer therapy. Arch Pharm Res 42: 159-170, 2019.
72. Grześ M, Jaiswar A, Grochowski M, Wojtyś W, Kaźmierczak W, Olesiński T, Lenarcik M, Nowak-Niezgoda M, Kołos M, Canarutto G, *et al*: A common druggable signature of oncogenic c-Myc, mutant KRAS and mutant p53 reveals functional redundancy and competition among oncogenes in cancer. Cell Death 15: 638, 2024.
73. Perurena N, Situ L and Cichowski K: Combinatorial strategies to target RAS-driven cancers. Nat Rev Cancer 24: 316-337, 2024.
74. Liu B, Zhou H, Tan L, Siu KTH and Guan XY: Exploring treatment options in cancer: Tumor treatment strategies. Signal Transduction Targeted Ther 9: 175, 2024.
75. Mattiuzzi C and Lippi G: Current cancer epidemiology. J Epidemiol Glob Health 9: 217-222, 2019.
76. De Angelis R, Demuru E, Baili P, Troussard X, Katalinic A, Chirlaque Lopez MD, Innos K, Santaquilani M, Blum M, Ventura L, *et al*: Complete cancer prevalence in Europe in 2020 by disease duration and country (EUROCARE-6): A population-based study. Lancet Oncol 25: 293-307, 2024.
77. Naqvi SZH, Kiran U, Ali MI, Jamal A, Hameed A, Ahmed S and Ali N: Combined efficacy of biologically synthesized silver nanoparticles and different antibiotics against multidrug-resistant bacteria. Int J Nanomedicine 8: 3187-3195, 2013.
78. Govindaraju K, Tamilselvan S, Kiruthiga V and Singaravelu G: Biogenic silver nanoparticles by Solanum torvum and their promising antimicrobial activity. J Biopesticides 3: 394-399, 2010.
79. Bhainsa KC and D'souza SF: Extracellular biosynthesis of silver nanoparticles using the fungus Aspergillus fumigatus. Colloids Surf B Biointerfaces 47: 160-164, 2006.
80. Ahmad A, Mukherjee P, Senapati S, Mandal D, Khan MI, Kumar R and Sastry M: Extracellular biosynthesis of silver nanoparticles using the fungus *Fusarium oxysporum*. Colloids Surfaces B: Biointerfaces 28: 313-318, 2003.
81. Jain N, Bhargava A, Majumdar S, Tarafdar J and Panwar J: Extracellular biosynthesis and characterization of silver nanoparticles using Aspergillus flavus NJP08: A mechanism perspective. Nanoscale 3: 635-641, 2011.
82. Zhang X, Yan S, Tyagi R and Surampalli RJC: Synthesis of nanoparticles by microorganisms and their application in enhancing microbiological reaction rates. Chemosphere 82: 489-494, 2011.
83. Al-Limoun M, Qaralleh HN, Khleifat KM, Al-Anber M, Al-Tarawneh A, Al-sharafa K, Kailani MH, Zaitoun MA, Matar SA and Al-soub T: Culture media composition and reduction potential optimization of mycelia-free filtrate for the biosynthesis of silver nanoparticles using the fungus *Tritirachium oryzae* W5H. Curr Nanosci 16: 757-769, 2020.
84. Khleifat K, Alqaraleh M, Al-Limoun M, Alfarrayeh I, Khatib R, Qaralleh H, Alsarayreh A, Al Qaisi Y and Abu Hajleh M: The ability of *Rhizopus stolonifer* MR11 to biosynthesize silver nanoparticles in response to various culture media components and optimization of process parameters required at each stage of biosynthesis. J Ecol Eng 23: 89-100, 2022.
85. Khleifat K, Qaralleh H and Al-Limoun M: Antibacterial activity of silver nanoparticles synthesized by *Aspergillus flavus* and its synergistic effect with antibiotics. J Pure Appl Microbiol 16: 1722-1735, 2022.
86. Abu Hajleh MN, Al-Limoun M, Al-Tarawneh A, Hijazin TJ, Alqaraleh M, Khleifat K, Al-Madanat OY, Qaisi YA, AlSarayreh A, Al-Samydai A, *et al*: Synergistic effects of AgNPs and biochar: A potential combination for combating lung cancer and pathogenic bacteria. Molecules 28: 4757, 2023.
87. Curman D, Cinel B, Williams DE, Rundle N, Block WD, Goodarzi AA, Hutchins JR, Clarke PR, Zhou BB, Lees-Miller SP, *et al*: Inhibition of the G2 DNA damage checkpoint and of protein kinases Chk1 and Chk2 by the marine sponge alkaloid debromohymenialdisine. J Biol Chem 276: 17914-17919, 2001.
88. Leirós M, Alonso E, Rateb ME, Houssen WE, Ebel R, Jaspars M, Alfonso A and Botana LM: Bromoalkaloids protect primary cortical neurons from induced oxidative stress. ACS Chem Neurosci 6: 331-338, 2015.
89. Jakubec P, Farley AJ and Dixon DJ: Towards the total synthesis of keramaphidin B. Beilstein J Org Chem 12: 1096-1100, 2016.
90. Lee SM, Kim NH, Lee S, Kim YN, Heo JD, Rho JR and Jeong EJ: (10 Z)-Debromohymenialdisine from marine sponge stylissa sp. regulates intestinal inflammatory responses in Co-culture model of epithelial Caco-2 cells and THP-1 macrophage cells. Molecules 24: 3394, 2019.
91. Abdullah N, Al Balushi N, Hasan SI, Al Bahlani S, Dobretsov S, Tamimi Y and Burney IA: Hymenialdisine is cytotoxic against cisplatin-sensitive but not against cisplatin-resistant cell lines. Sultan Qaboos Univ Med J 21: 632-634, 2021.
92. Ueda G, Matsuo Y, Murase H, Aoyama Y, Kato T, Omi K, Hayashi Y, Imafuji H, Saito K, Tsuboi K, *et al*: 10Z-Hymenialdisine inhibits angiogenesis by suppressing NF-κB activation in pancreatic cancer cell lines. Oncol Rep 47: 48, 2022.
93. Esposito R, Federico S, Glaviano F, Somma E, Zupo V and Costantini M: Bioactive compounds from marine sponges and algae: Effects on cancer cell metabolome and chemical structures. Int J Mol Sci 23: 10680, 2022.
94. El-Naggar HA, Bashar MA, Rady I, El-Wetidy MS, Suleiman WB, Al-Otibi FO, Al-Rashed SA, Abd El-Maoula LM, Salem EL-S, Attia EMH, *et al*: Two red sea sponge extracts (*Negombata magnifica* and *Callyspongia siphonella*) induced anticancer and antimicrobial activity. Applied Sci 12: 1400, 2022.
95. Murugesan A, Mani SK, Koochakkhani S, Subramanian K, Kandhavelu J, Thiyagarajan R, Gurbanov AV, Mahmudov KT and Kandhavelu M: Design, synthesis and anticancer evaluation of novel arylhydrazones of active methylene compounds. Int J Biol Macromol 254: 127909, 2024.
96. Ramezani-Aliakbari M, Soltanabadi A, Sadeghi-aliabadi H, Varshosaz J, Yadollahi B, Hassanzadeh F and Rostami M: Eudesmic acid-polyoxomolybdate Organo-conjugate as novel anticancer agent. J Mol Structure 1240: 130612, 2021.
97. Cuenya BR and Behafarid F: Nanocatalysis: Size-and shape-dependent chemisorption and catalytic reactivity. Surface Sci Rep 70: 135-187, 2015.
98. Lakkim V, Reddy MC, Pallavali RR, Reddy KR, Reddy CV, Inamuddin, Bilgrami AL and Lomada D: Green synthesis of silver nanoparticles and evaluation of their antibacterial activity against multidrug-resistant bacteria and wound healing efficacy using a murine model. Antibiotics (Basel) 9: 902, 2020.
99. Rahman NIA, Ramzi MM, Rawi NN, Siong JYF, Bakar K, Bhubalan K, Ariffin F, Saidin J, Azemi AK and Ismail N: Characterization of antibiofilm compound from marine sponge *Stylissa carteri*. Environ Sci Pollut Res Int 31: 37552-37563, 2024.
100. Hawas UW, Shaher F, Ghandourah M, Abou El-Kassem LT, Satheesh S and Al-Sofyani AMA: Lipids and free fatty acids of Red Sea Avrainvillea amadelpha, Holothuria atra, and *Sarcocornia fruticosa* inhibit marine bacterial biofilms. Lett Organic Chemistry 17: 466-471, 2020.
101. Hamed AN, Schmitz R, Bergermann A, Totzke F, Kubbutat M, Müller WEG, Youssef DTA, Bishr MM, Kamel MS, Edrada-Ebel R, *et al*: Bioactive pyrrole alkaloids isolated from the Red Sea: Marine sponge *Stylissa carteri*. Z Naturforsch C J Biosci 73: 199-210, 2018.

102. Althagbi HI, Alarif WM, Al-Footy KO and Abdel-Lateff A: Marine-derived macrocyclic alkaloids (MDMAs): Chemical and biological diversity. Mar Drugs 18: 368, 2020.
103. Júnior ACV, de Castro Nogueira Diniz Pontes M, Barbosa JP, Höfling JF, Araújo RM, Boniek D, de Resende Stoianoff MA and Andrade VS: Antibiofilm and Anti-candidal activities of the extract of the marine sponge agelas dispar. Mycopathologia 186: 819-832, 2021.
104. Al-Shamayleh W, Qaralleh H, Al-Madadheh OA, Al Qaisi Y and AlSarayreh A: Inhibitory effect of the marine sponge amphimidon chloros extracts against multidrug-resistant bacteria. Tropical J Natural Product Res: 8, 2024.
105. Barbosa F, Pinto E, Kijjoa A, Pinto M and Sousa E: Targeting antimicrobial drug resistance with marine natural products. Int J Antimicrob Agents 56: 106005, 2020.
106. Chen S, Liu D, Zhang Q, Guo P, Ding S, Shen J, Zhu K and Lin W: A marine antibiotic kills multidrug-resistant bacteria without detectable high-level resistance. ACS Infect Dis 7: 884-893, 2021.
107. Schneider YK: Bacterial natural product drug discovery for new antibiotics: strategies for tackling the problem of antibiotic resistance by efficient bioprospecting. Antibiotics (Basel) 10: 842, 2021.
108. Jacob MR, Hossain CF, Mohammed KA, Smillie TJ, Clark AM, Walker LA and Nagle DG: Reversal of fluconazole resistance in multidrug efflux-resistant fungi by the dysidea a renaria sponge sterol 9α, 11α-epoxycholest-7-ene-3β, 5α, 6α, 19-tetrol 6-acetate. J Nat Prod 66: 1618-1622, 2003.
109. Saravanakumar K, Abinaya M, Mehnath S, Shanmuga Priya V, Jeyaraj M, Al-Rashed S and Muthuraj V: Nano Ag@ bioactive microspheres from marine sponge clathria frondifera: Fabrication, fortification, characterization, anticancer and antibacterial potential evaluation. Environ Res 206: 112282, 2022.
110. Bayona LM, de Voogd NJ and Choi YH: Metabolomics on the study of marine organisms. Metabolomics 18: 17, 2022.